EVALUATION OF AGED TRANSFORMER OILS BY MICROWAVE ABSORPTION MEASUREMENTS

by

EDGAR HENRY SCHROEDER

B.A.Sc., The University of British Columbia, 1962

A THESIS SUBMITTED IN PARTIAL FULFILMENT OF THE REQUIREMENTS FOR THE DEGREE OF

MASTER OF APPLIED SCIENCE

in the Department of

Electrical Engineering

We accept this thesis as conforming to the standards required from candidates for the degree of Master of Applied Science

Members of the Department
of Electrical Engineering

THE UNIVERSITY OF BRITISH COLUMBIA

June 1964

In presenting this thesis in partial fulfilment of the requirements for an advanced degree at the University of British Columbia, I agree that the Library shall make it freely available for reference and study. I further agree that permission for extensive copying of this thesis for scholarly purposes may be granted by the Head of my Department or by his representatives. It is understood that copying or publication of this thesis for financial gain shall not be allowed without my written permission.

Department of Electrical Engineering

The University of British Columbia,
Vancouver 8, Canada

Date July 7, 1964.

ABSTRACT

The deterioration of electrical insulating oils results in the formation of complex oxidation products, many of which are polar in structure. The significance of the microwave-frequency dielectric-loss measurement, when applied to the evaluation of aged transformer oils, is investigated.

A cylindrical cavity, operating in the TE_{01} mode, is used to measure the loss tangent of aged transformer oils. Q-factor measurements are made by a dynamic method which is described. The problem of mode interference in the cavity is investigated in detail.

It is found that the loss tangent of transformer oils, measured at X-band, increases as the oil deteriorates through oxidation. The increase is influenced by several factors but closely parallels the increase in acidity. Sludge particles do not in themselves cause a significant increase in the dielectric losses. An indirect correlation between the loss tangent and the sludge content of an oil may exist but has not been established.

The change in the dielectric constant of an oil caused by the presence of dissolved water, or by the ageing process, is too small to be measured by the method used. A small but measureable increase in the loss tangent is produced by the presence of water in concentrations of approximately 75 parts per million.

ACKNOWLEDGEMENT

The writer wishes to convey his sincere thanks to his supervisor, Dr. W. A. G. Voss, for the many valuable discussions and for his interest, encouragement and enthusiasm throughout the duration of the work.

Acknowledgement is gratefully given to the National Research Council for the financial assistance received from a Bursary awarded in 1962, a Studentship in 1963 and funds for research through the Departmental Grant, BT-68.

Special thanks are extended to Dr. F. Noakes for suggestions from which the project evolved. The assistance received from Dr. I. H. Warren of the Department of Metallurgy, Mr. J. A. Forster of B. C. Hydro and Power Authority and Mr. E. K. Lewis of Imperial Oil Enterprises Limited is greatly appreciated.

The author also wishes to thank his colleagues, particularly Mr. D. R. McDiarmid, for the interesting and helpful discussions.

TABLE OF CONTENTS

LIST OF ILLUSTRATIONS

LIST OF TABLES

1. INTRODUCTION

1.1. Review of Information on Transformer Oils

Refined petroleum oils have good electrical insulating properties and are widely used as liquid dielectrics in transformers, switch gear and power cables. However, each type of application places its own special demands upon certain properties of the oil.

For the case of transformers, power dissipation causes a considerable increase in temperature and the oil must act as a heat-transfer fluid in addition to its role as an insulator. For this reason, chemically stable oils with high oxidation resistance are required if satisfactory service life is to be obtained. The elevated temperatures encountered in normal service tend to accelerate deterioration of the oil so that, in time, it must be replaced or reclaimed in order to avoid service failure and equipment damage.

Transformer oils have an indefinite chemical composition dependent upon the type of crude from which they are produced and also on the refining process selected for their manufacture. Both saturated and unsaturated hydrocarbons are usually present so that the oil is a complex mixture containing various amounts of napthenes, paraffins and aromatics. Olefins and other easily oxidized substances are removed by the refining process since the presence of such components would confer a low chemical stability on the oil. Transformer oils used in Canada are primarily napthenic. Because specifications

require them to pour at minus 50°F, they are manufactured from imported, wax-free, napthenic-base crudes.(1)

From an engineering viewpoint, the harmful symptoms of transformer oil deterioration in service are:

(a) A decrease in breakdown voltage caused mainly by the presence of moisture and fibres,

(b) The formation of sludge which deposits on various parts of the transformer and hinders normal heat dissipation,

(c) The formation of acidic products which may damage solid insulation or cause metal corrosion in the transformer.

Moisture and fibres are present as impurities and can be removed by drying and filtering or by centrifuging.

The acids and sludges are formed by oxidation of the hydrocarbon constituents of the oil. This process is accelerated by the increased temperature and the presence of oxidation promoters and certain catalysts. A large volume of literature has been devoted to a study of oil oxidation, a review of which is given by Morton(2). Several metals, of which copper is the most important, act as catalysts during oxidation.(3) These catalytic effects occur in all transformers but can be greatly reduced by the proper use of anti-oxidants or inhibitors.(4)

The oxidation reactions are complex and only a few general conclusions may be drawn. The products formed, particularly the acids and sludges, are related to the nature of the oil

undergoing oxidation, the type of catalyst present, the temperature at which the oxidation takes place and the amount of oxygen available for reaction. Oils which have been heavily refined to remove aromatics are readily oxidized to form acidic products but give virtually no sludge. Less heavily refined oils which still retain a portion of their original aromatic hydrocarbon content are more resistant to oxidation and do not show this tendency toward acid development. However, they will produce more sludge. Inhibitors, when added to good quality oils which have been properly refined, are very effective in retarding acid and sludge formation. They are much less effective when added to low quality oils which contain oxidation promoters or those from which the natural inhibitors have been removed by over-refining.

Because of their complex composition, transformer oils are subjected to a large number of tests in an effort to evaluate their quality and suitability for service. Specifications for insulating oils usually call for tests of such physical, chemical and electrical properties as pour point, color, viscosity, volatility, specific gravity, flash point, neutralization number or acidity, free and corrosive sulphur content, interfacial tension against water, oxidation stability, dielectric strength and power factor.

The oxidation stability test is used to measure the sludge and acid-forming tendencies of a new oil. Although no definite correlation has been established between laboratory

oxidation tests and service life, these tests are more useful than any other in judging the quality of a new oil and predicting its future deterioration. In the commonly used tests of this type, oil samples are subjected to an oxidizing atmosphere at a specified temperature and after specified time intervals, the accumulation of acid and sludge is measured.

1.2. Testing of Oils in Service

Maintenance procedures require tests capable of measuring the deterioration of an oil which has been in service for some time. The tests normally used for this purpose are chosen from the specification or acceptance tests and include neutralization number, interfacial tension, color, dielectric strength, power factor, resistivity and oxidation life tests. A rough indication of when the oil should be changed can be obtained but none of these tests is entirely satisfactory.

Oxidation tests which measure sludge accumulation are sometimes applied to determine the useful life remaining in an oil. Some oils, particularly inhibited oils, have a definite initial induction period during which oxidation proceeds very slowly, followed by a period of more rapid deterioration. In such cases, the length of the induction period which remains can be measured by oxidation tests but they are generally of little value when applied to the more commonly used uninhibited oils. After an extensive field-testing program which lasted ten years, McConnell[5] concluded that the sludge-accumulation test, when carried out on uninhibited oils that have been

subjected to service, cannot be considered acceptable as an indication of oil quality at that time or its fitness for further service. He stated that the most useful tests for this purpose are the neutralization number, interfacial tension and color.

The neutralization number refers to the amount of potassium hydroxide (KOH) required to neutralize one gram of oil and is thus a measure of the acidity of the oil. Interfacial tension values are highest for a new oil and decrease rapidly to a low value which is approached asymptotically as the oxidation progresses. This test measures the amount of surface-active intermediate products of oxidation present and is of value only during the early stages of oil deterioration. Color, when considered by itself, is misleading in evaluating oils of service quality but can be helpful in conjunction with other tests.

None of the foregoing tests can be considered as a reliable indicator of how much sludge is likely to be found in a transformer. However, experience in the field has shown that oils do not usually develop a significant amount of sludge until their acidities have reached a certain level. In Britain, it is considered unwise to leave an oil in service when its acidity has reached a value of 1.0 mg KOH per gram. Low values of interfacial tension are measured well before significant sludge formation occurs and this test is found to be of no value.[6] Oliver[7] has pointed out that in the United States, most operators of power transformers consider

oil suitable for service when the acidity is less than some arbitrary value in the 0.4 to 0.7 mg KOH per gram range. With this decreased limit placed on acidity, interfacial tension values have more significance and are often used in conjunction with neutralization numbers.

The breakdown voltage of an insulating oil depends primarily on the degree of contamination by fibres and moisture. The dielectric strength test is only a measure of such contamination and is a very unsatisfactory criterion for the condition of an oil which has been in service.

1.3. The Low-Frequency Power-Factor Test

The low-frequency power-factor test is often used as a criterion for oil quality, particularly with reference to cable and capacitor oils. It has also been used to measure the deterioration of transformer oils in the field, replacing both neutralization number and interfacial tension values in determining the need for oil reclamation.

In its simplest form, the power-factor test consists of filling a capacitor with oil and comparing the dielectric losses with those of a standard capacitor whose losses are accurately known. A type of Schering bridge is used for the comparison and very strict attention must be paid to cleanliness of the test cell and other details in order to obtain repeatable results.[8][9][10] The test is normally carried out at a temperature between 20°C and 100°C at power-line frequency. Under these conditions, polarization losses

in the oil are negligible and the power-factor test is essentially a measurement of oil conductivity or resistivity.

The actual value of oil conductivity is of importance only for cable and capacitor oils where low conductivity is required in order to prevent overheating through ohmic losses. For transformer oils, the actual value of oil conductivity is usually not significant but it is of interest if it can be correlated to other important properties of the oil. Attempts have been made to correlate conductivity and power-factor values with such properties as acid and sludge content. At best, such correlations are poor because conductivity is very much dependent upon the presence of certain trace impurities.

Childs and Stannet[11] used resistivity and acidity tests to evaluate the condition of transformer oils in service. The conductivity was found to depend strongly on the total iron content of the oils as well as upon acidity. For an oil with an acidity of 0.2 mg KOH per gram, an increase in iron content from 0.1 to 10 parts per million caused a tenfold increase in conductivity. There was no apparent connection between the occurrence of iron and acidity in the oils. The large effect of traces of iron on conductivity is also discussed by Salomon[12]. He found that artificially ageing a new transformer oil for 48 hours at 115°C, in the presence of an iron wire, increased the conductivity of the oil by a factor of 1000. Other trace impurities also had large effects. After many ageing experiments he concluded that there is no quantitative correlation between the increase in power factor and the sludge value or acidity produced. Bennett[10] gives a graph

illustrating the large effect which the presence of moisture has on the resistivity of an oil. McConnell[5] states that power factor and dc resistivity measurements made on transformer oils, during his program of field testing, appeared to have little or no significance.

From these and similar experiments, one is led to the conclusion that neither the low-frequency power-factor test nor the dc resistivity test is of much value in determining the condition of a transformer oil in service.

1.4. Object of the Work

Transformer oils which have been properly refined are almost entirely free from polar molecules. When put into service they become subject to polar contamination because many of the important deterioration products formed as a result of oxidation have molecules which are polar in structure. It should therefore be possible to evaluate the condition of an oil by measuring the polarization losses associated with the deterioration products. A high degree of deterioration would be indicated by large losses.

Debye[13] has shown that for dilute solution of polar molecules in nonpolar liquids, the relaxation time of the dipoles is given approximately by the expression

$$\tau_d = \frac{4\pi \eta r^3}{kT} \qquad \ldots 1.1$$

where η is the viscosity of the liquid, r is the radius of the spherical dipole, k is Boltzmann's constant and T is the absolute temperature. The orientational polarization losses

are a maximum at an angular frequency, $\omega = \frac{1}{\tau_d}$. From Equation 1.1 it follows that for ordinary temperatures, permanent dipoles of atomic dimensions ($r = 1$ Å) have a relaxation time of approximately 10^{-10} sec when in a liquid such as transformer oil. As a result, the maximum orientational polarization losses should occur at frequencies near 10^9 c/s. Due to the large number of different oxidation products formed, the loss peak is probably very broad with significant losses occurring throughout the microwave spectrum.

This thesis uses a microwave technique to investigate the correlation between the deterioration of transformer oil and the resultant increase in dielectric losses measured at X-band. The purpose of the investigation is to determine the significance of the dielectric-loss measurement at microwave frequency when used as a criterion of quality for oils in service.

In previous work done in this Department, Smith[14] used lumped-parameter circuits to measure the dissipation factor of transformer oil at various temperatures and at frequencies up to 10 Mc/s. One of his conclusions was that the dispersion method for testing transformer oils, in the frequency spectrum 20 c/s to 10 Mc/s and at room temperature, was not satisfactory. However, his measurements did indicate that at room temperature, the maximum in the dissipation factor could be expected to occur at very high frequency.

1.5. Classical Theory of Dielectric Losses

The relation between the electric displacement D, the electric field E and the polarization P is given by

$$D = \epsilon_o E + P \qquad \ldots 1.2$$

where ϵ_o is the permittivity of free space. For linear dielectrics, the polarization is a linear function of the electric field and Equation 1.2 may be written as $D = \epsilon E$, where ϵ is the permittivity of the material and is given by

$$\epsilon = \epsilon_o + \frac{P}{E} \qquad \ldots 1.3$$

The ratio of the polarization to the electric field, $\frac{P}{E}$, is the electric susceptibility χ. In general, χ is frequency dependent and it is this fact which gives rise to the familiar polarization losses.

The polarization which occurs when a dielectric is subjected to an external electric field may be considered as the sum of three contributions:

$$P = P_e + P_a + P_d \qquad \ldots 1.4$$

The subscripts e, a and d refer respectively to electronic, atomic and dipolar polarization. The electronic polarization results from an elastic displacement of the electron cloud of an atom relative to the nucleus. The atomic polarization is caused by changes in bond angles or interatomic distances of atoms within the molecule as a result of the applied field. Molecules which have a permanent dipole moment will attempt to align themselves in the direction of the applied field. This latter effect is known as dipolar or orientational polarization.

All of the foregoing mechanisms lead to dielectric losses but their individual contributions to the total losses are important in different parts of the frequency spectrum. The

relaxation time, τ_e or τ_a, associated with electronic and atomic polarization is of the order of 10^{-13} to 10^{-15} sec. Since the maximum losses occur at angular frequencies such that $\omega\tau = 1$, the dielectric losses caused by these polarizations are important in the infrared to ultraviolet range but are small at lower frequencies. Depending on the nature of the material, the relaxation time of permanent dipoles may be somewhere between days and 10^{-12} sec. For many slightly polar dielectrics, τ_d is approximately 10^{-9} or 10^{-10} sec and these dielectrics have a loss peak in the microwave region of the frequency spectrum.

From Equations 1.3 and 1.4, the permittivity of a dielectric may be written as

$$\varepsilon = \varepsilon_o + \chi_e + \chi_a + \chi_d \qquad \ldots 1.5$$

The frequency dependence of each electric susceptibility can be crudely approximated by assuming it to be of the form

$$\chi_i = \frac{\chi_{io}}{1 + j\omega\tau_i},$$

where the subscript i, refers to either e, a or d. From the magnitude of the appropriate relaxation times, it follows that the electronic and atomic polarizations contribute their full share to the total polarization at microwave frequencies. Referring to Figure 1.1, a high-frequency permittivity ε_{ea} may be defined as $\varepsilon_{ea} = \varepsilon_o + \chi_e + \chi_a$. A static or zero-frequency permittivity ε_s can be defined as $\varepsilon_s = \varepsilon_{ea} + \chi_{do}$. Using these definitions, Equation 1.5 becomes

$$\varepsilon = \varepsilon_{ea} + \frac{\varepsilon_s - \varepsilon_{ea}}{1 + j\omega\tau_d} \qquad \ldots 1.6$$

Thus, the frequency dependence of the electric susceptibility can be described by introducing the concept of a complex permittivity ϵ_c written as

$$\epsilon_c = \epsilon' - j\epsilon'' \qquad \ldots 1.7$$

where, from Equation 1.6,

$$\epsilon' = \epsilon_{ea} + \frac{\epsilon_s - \epsilon_{ea}}{1 + \omega^2\tau_d^2} \qquad \ldots 1.8$$

$$\epsilon'' = (\epsilon_s - \epsilon_{ea}) \frac{\omega\tau_d}{1 + \omega^2\tau_d^2} \qquad \ldots 1.9$$

These two equations are referred to as the Debye Equations[15]. The ratio ϵ'/ϵ_o is defined as the relative permittivity ϵ_r, also known as the dielectric constant. The ϵ'' term is responsible for the dielectric losses.

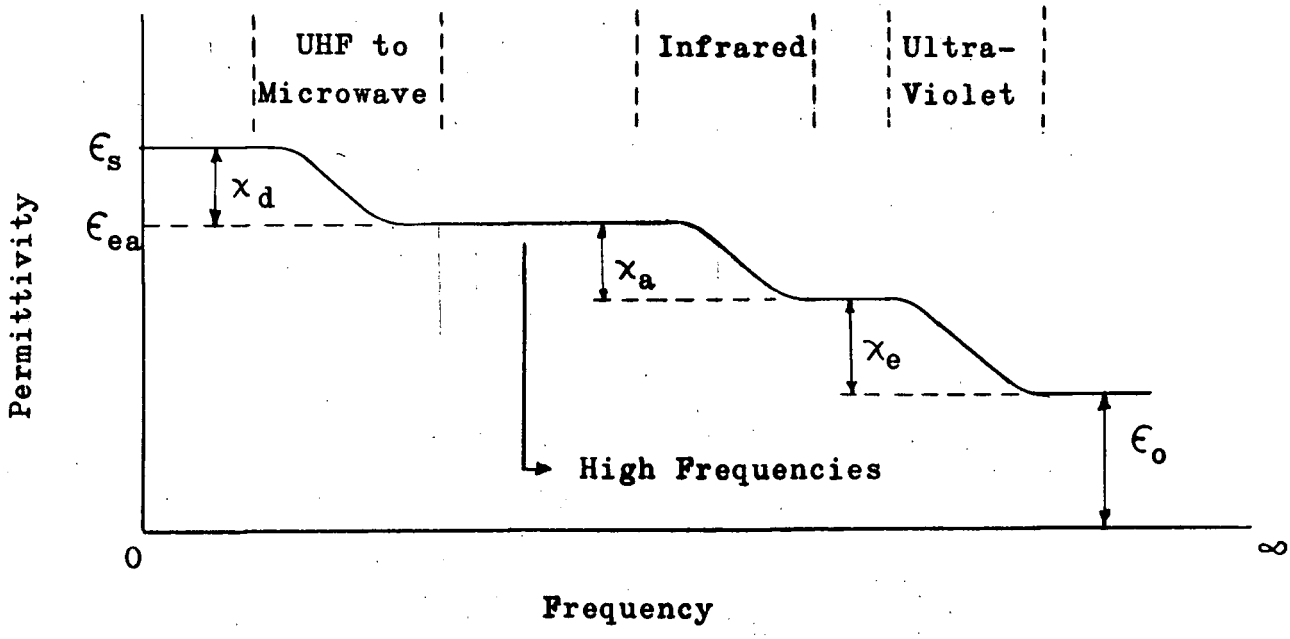

Fig. 1.1 Frequency Dependence of Permittivity

When a dielectric of permittivity ϵ_c is placed in a time-varying electric field $E = E_o e^{j\omega t}$, a current flows. Defining σ as the conductivity of the dielectric, the total current density J_T is written as, taking $D = \epsilon_c E$,

$$J_T = \sigma E + \frac{\partial D}{\partial t} = (\sigma + \omega\epsilon'')E + j\omega\epsilon' E \quad \ldots 1.10$$

The component of the current which is in phase with E results in power dissipation. The average power loss w, per unit volume, is

$$w = \frac{1}{2}(\sigma + \omega\epsilon'')\, E_o^2 \quad \ldots 1.11$$

The maximum stored-energy density in the dielectric is equal to $\frac{1}{2}\epsilon' E_o^2$. Hence, defining the Q of the dielectric in the usual way and taking $\sigma = 0$ for simplicity,

$$Q = \omega \frac{\text{Maximum Stored Energy}}{\text{Average Power Loss}} = \frac{\epsilon'}{\epsilon''} \quad \ldots 1.12$$

The reciprocal of the Q-factor is referred to as the loss tangent or tan δ and is given by

$$\tan \delta = \frac{\epsilon''}{\epsilon'} \quad \ldots 1.13$$

In writing Equations 1.12 and 1.13, σ has been set equal to zero in order to simplify the equations. However, these equations may still be regarded as perfectly general for all dielectrics provided the quantity ϵ'' is redefined to include the effects of non-zero conductivity. Referring to Equation 1.9, this is done by adding a term $\frac{\sigma}{\omega}$ to account for the conductivity. With this new definition of ϵ'', the total current density is written as

$$J_T = (\omega\epsilon'' + j\omega\epsilon')E \quad \ldots 1.14$$

The quantity ε'' now includes terms for all the mechanisms giving rise to currents which are in phase with the applied field and, with this definition of ε'', the generality of Equations 1.12 and 1.13 follows.

At very low frequencies, polarization losses are negligible so that $\varepsilon'' = \frac{\sigma}{\omega}$. Therefore, $\tan \delta = \frac{\varepsilon''}{\varepsilon'} = \frac{\sigma}{\omega \varepsilon'}$, which is the familiar ratio of conduction current to displacement current in a capacitor. As the frequency is increased, the polarization losses also increase, pass through a maximum and then decrease once more to a low value. In the experiments, the dielectric losses at X-band are due primarily to polarization effects.

2. THE MEASUREMENT TECHNIQUE AT X-BAND FREQUENCY

2.1. Choice of a Method

Transformer oils in their initial state have values of tan δ and dielectric constant of the order of 0.001 and 2.1 respectively. Although the deterioration of an oil was expected to be accompanied by an increase in tan δ, the magnitude of the increase which would occur was not known. In choosing a measurement technique, two basic requirements were considered to be of primary importance:

(a) The method must be capable of making accurate and repeatable measurements of tan δ and dielectric constant in the range of interest.

(b) The experimental procedure involved in making a measurement should be as simple and direct as possible.

Both waveguide and resonant-cavity methods are used for measurements on medium-loss dielectrics. In waveguide methods, a section of the guide is sealed and filled with the specimen under test, thus serving as an absorption cell. By terminating the cell with an open-circuit or short-circuit and comparing the VSWR and the positions of the voltage nodes in the input waveguide for the cases of the empty and the filled cell, the values of tan δ and dielectric constant of the sample may be deduced. A simplification of the procedure can be made by adjusting the length of the absorption cell, or alternatively, the excitation frequency, so that an integral number of half

wavelengths occurs in the cell. In this quasi-resonant method, only the specimen length and the VSWR in the input guide are required for a determination of tan δ. Many sources of error must be taken into account with the result that accuracies are generally not comparable to those obtainable with resonant-cavity techniques. The foregoing waveguide methods have been discussed in detail by Luthra and Walker[16] who applied them to ceramics.

Cavity methods are well suited to measurements on medium and low-loss dielectrics. The dielectric sample is placed into the cavity which is coupled to the input waveguide and excited into the desired mode of resonance. In order to calculate the loss tangent and the dielectric constant is is necessary to measure the depth of dielectric in the cavity, the length of the empty cavity at resonance, the length of the cavity at resonance with the dielectric in place and the Q-factors of the cavity, both in the absence and presence of the dielectric. For low-loss liquid dielectrics, the cavity may be completely filled, in which case the calculations are particularly simple. In almost all instances the effect of wall losses can be accounted for more readily than in corresponding waveguide methods with the result that greater accuracy is obtainable.

Q measurements can be conveniently made utilizing a sophisticated dynamic method described by Free[17]. In spite of the relatively large amount of equipment which is required for tests, the experimental procedure is simple and yields good results.

Due to these considerations, a resonant-cavity technique was chosen and used for all tan δ and dielectric constant measurements. For reasons discussed in a later section it was found impractical to use a completely filled cavity for tan δ measurements but good results were obtained using the partly filled cavity. The method for Q measurement will now be described.

2.2. Apparatus for Q Measurement

A block diagram of the equipment is shown in Figure 2.1. An air-cooled klystron oscillator is frequency modulated by the superposition of a sawtooth voltage from the CRO sweep onto the reflector voltage. The cavity, used as a transmission device, is loosely coupled to the input waveguide and is tuned to resonate at the centre frequency of the klystron. At the output of the cavity, the transmission resonance curve is detected, amplified by a low-noise audio amplifier and displayed on one trace of a dual-beam oscilloscope. The Q-factor of the cavity is determined by measuring the frequency separation of the resonance curve half-power points. This measurement is easily and accurately made using markers of known frequency separation that are displayed on the second trace of the oscilloscope.

Generation of the frequency markers is accomplished by a straight-forward double-heterodyne method. By means of the directional coupler and hybrid-T junction, a small portion of the output power from the frequency-modulated klystron is transferred to the first crystal mixer. Here it is heterodyned

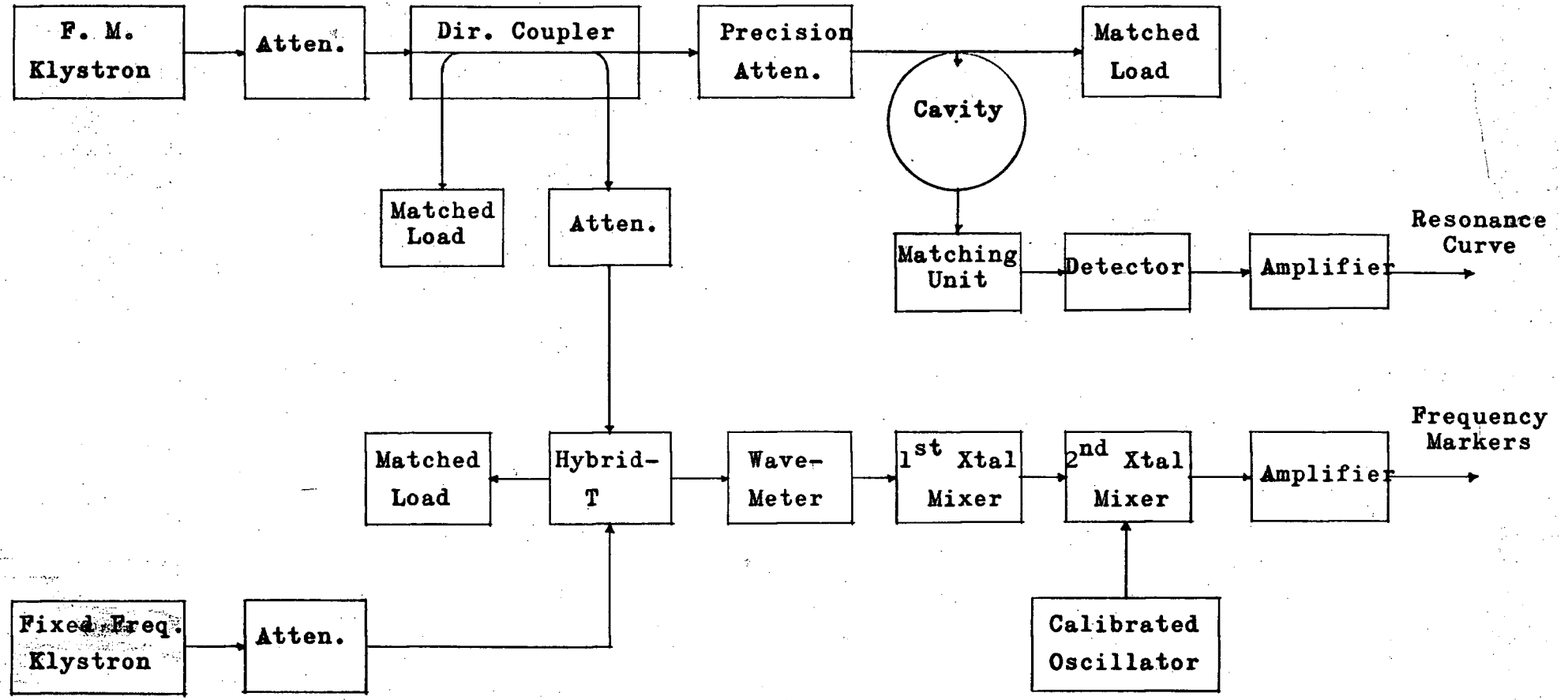

Fig. 2.1 Block Diagram of Apparatus

with the output of an unmodulated, fixed-frequency klystron tuned approximately to the centre frequency of the first. The mixer output consists of a frequency-modulated signal corresponding to the difference frequency between the two klystrons. This signal is now combined with the output of a calibrated oscillator in a second crystal mixer. After amplification of the output and removal of high-frequency components, three markers are available. The centre marker is produced when the klystrons are in tune and the outer two when they differ by the oscillator frequency.

Additional smaller markers, corresponding to harmonics of the oscillator frequency, are produced if the power levels at the mixer inputs are not correctly adjusted. These extra markers will not be present if the circuits have been well adjusted but, in any case, they are small and cause no confusion even if they are visible.

The markers may be moved as a group in a horizontal direction on the CRO trace by slightly adjusting the frequency of the second klystron. A fine control of the reflector voltage is a good method of achieving this smoothly. The separation of the outer markers is controlled by adjusting the frequency of the calibrated oscillator. The photographs of Figure 2.2 illustrate the quality of the traces and markers available, as well as the use of the markers and precision attenuator in measuring the frequency separation of the resonance curve half-power points.

The procedure for Q measurement is as follows. The

cavity is first tuned until the peak of the resonance curve occurs at the centre frequency of the swept klystron. The vertical position of the oscilloscope trace upon which the markers are displayed is adjusted until it is located at the peak of the resonance curve. The input power to the cavity is now doubled by adjusting the precision attenuator. After readjusting the resonance curve baseline to its original level, the markers occur at the half-power level on the vertical scale. By making the necessary width and horizontal position adjustments, the markers are superimposed on the resonance curve half-power points whose frequency separation can now be determined directly from the scale setting of the calibrated oscillator.

Important advantages are gained by using this technique for Q measurement:

(a) The measured Q-factor is independent of the crystal detector characteristics.

(b) Slight instability of the klystron frequency during the measurement does not affect the accuracy of the result. If small frequency drifts occur, they are seen as slight horizontal shifts of the resonance curve on the oscilloscope trace. The shape of the resonance curve is left unchanged.

(c) Measurements are rapid and easy to make.

The chief disadvantage of the technique is that the power output of the klystron may not remain constant over the swept-frequency band. In later experiments it was found that this

effect was appreciable and a correction had to be applied.

2.3. Design of the Cavity

For the accurate determination of dielectric losses by cavity methods, the mode choice and cavity design are necessarily such that wall losses are small compared with specimen losses. This allows the dielectric losses to be calculated by measuring the total losses in the cavity and then applying a correction term for the resistive losses on the walls. Assuming that this correction term can be calculated to an accuracy of about 90%, the uncertainty introduced into loss tangent values will not exceed 1.5% if the cavity wall losses are less than 15% of the specimen losses. This argument leads to the conclusion that a cavity with a Q_o value of not less than 15,000 is required for loss tangent measurements with a partly filled cavity whose measured Q is about 3000.

A cylindrical cavity designed to operate at 8.5 Gc/s in the TE_{01} mode was used for the measurements. The photograph of Figure 2.3 shows the cavity and some of the associated equipment.

The TE_{01} mode of operation was chosen because of the highly desirable field pattern associated with this mode. Since the E-field is purely circumferential, there is no current flow between the side wall and the end wall of the cavity. Hence, the cavity may be tuned by a non-contacting plunger which helps to damp out undesired modes of resonance. A further desirable property of the TE_{01} mode is that the

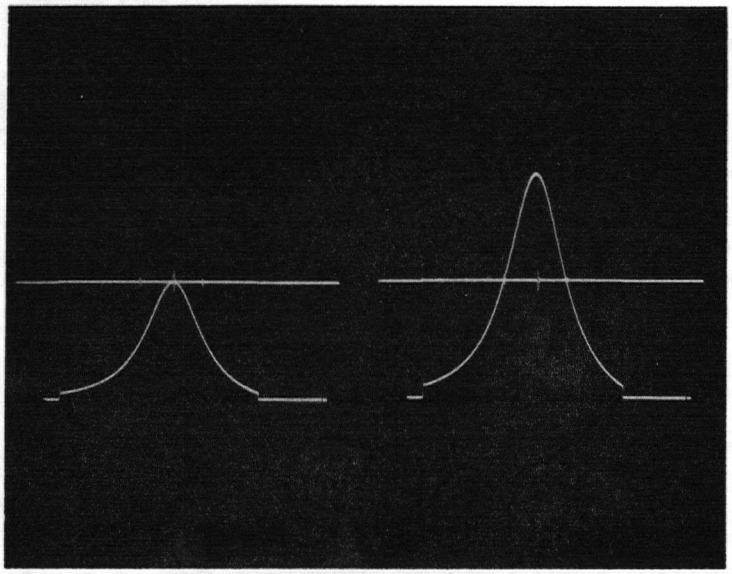

Fig. 2.2 Resonance Curve and Markers

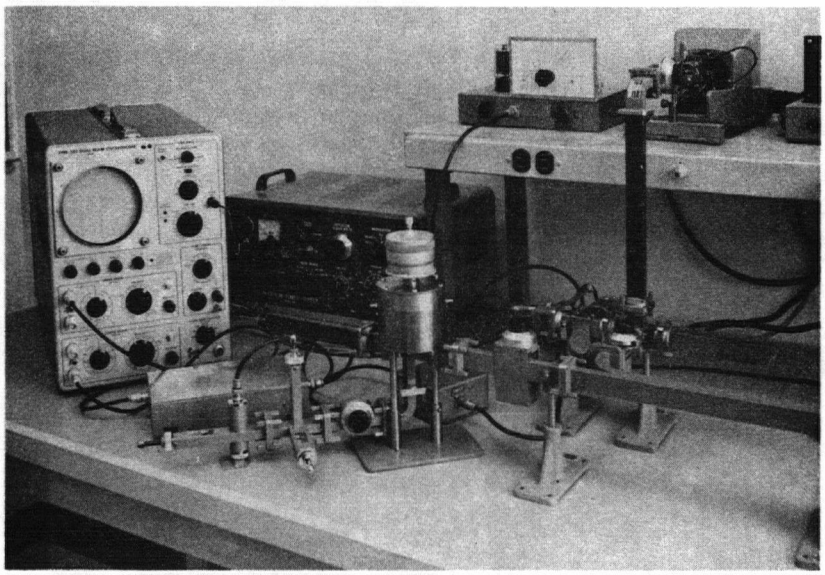

Fig. 2.3 Cavity and Associated Equipment

fields have no azimuthal dependence. As a result, the TE_{01} mode is a singlet and has no tendency to split or become unstable due to small irregularities in the cavity. The fact that the TM_{11} mode is a companion mode of the TE_{01} is not a serious disadvantage. The coupling elements can be located to excite the desired mode preferentially. In addition, the undesired TM_{11} mode is strongly perturbed by the presence of the gap at the tuning plunger.

The cavity was made entirely of brass. Choosing a diameter of 3.090 inches and a maximum length of 2.6 inches gave a Q_o value in the desired range without plating the cavity. The tuning plunger position was controlled by a micrometer screw of length one inch, calibrated to 0.0001 inch. In order to permit plunger travel over a distance larger than one inch, the cavity barrel was made in two sections, the upper one being easily removed. This permitted the cavity length to be varied by the plunger from 0.7 to 2.6 inches, a range sufficient to locate the first three resonances of the TE_{01} mode in the air-filled cavity.

Originally the base plate was fastened to the cavity by machine screws and was sealed by a gasket. This arrangement was inconvenient for two reasons:

(a) The gasket was somewhat compressible. Therefore the length of the cavity as measured by the micrometer depended upon the tension of the base-plate mounting screws.

(b) The presence of the gasket made cleaning of the cavity difficult.

For these reasons, the base plate was securely fastened to the cavity barrel and permanently soldered into place. A small hole near the outer perimeter of the base plate served as a drain.

2.4. The Coupling Arrangement

For a uniform waveguide system, the guide wavelength λ_g, the free-space wavelength λ_o and the cut-off wavelength λ_c are related by the equation

$$\frac{1}{\lambda_g^2} = \epsilon_r \frac{1}{\lambda_o^2} - \frac{1}{\lambda_c^2} \qquad \ldots 2.1$$

The cut-off wavelengths for TE_{nm} and TM_{nm} waves in a cylindrical waveguide are given by

$$TE_{nm}: \quad \lambda_c = \frac{2\pi a}{K_{nm}}$$

$$TM_{nm}: \quad \lambda_c = \frac{2\pi a}{S_{nm}} \qquad \ldots 2.2$$

In these expressions, a is the radius of the guide; K_{nm} is the m^{th} root of $J_n'(x) = 0$; S_{nm} is the m^{th} root of $J_n(x) = 0$.

At a frequency of 8.5 Gc/s, a cavity of diameter 3.090 inches will propagate any mode for which the ratio of cut-off wavelength to guide radius, $\frac{\lambda_c}{a}$, is greater than 0.9. Thus, thirteen modes of propagation are possible in the air-filled cavity. Filling the cavity with dielectric results in additional modes of propagation being permitted. In order to excite the desired TE_{01} mode preferentially, the coupling configuration used by Bleaney[18] and illustrated schematically in Figure 2.4 was employed.

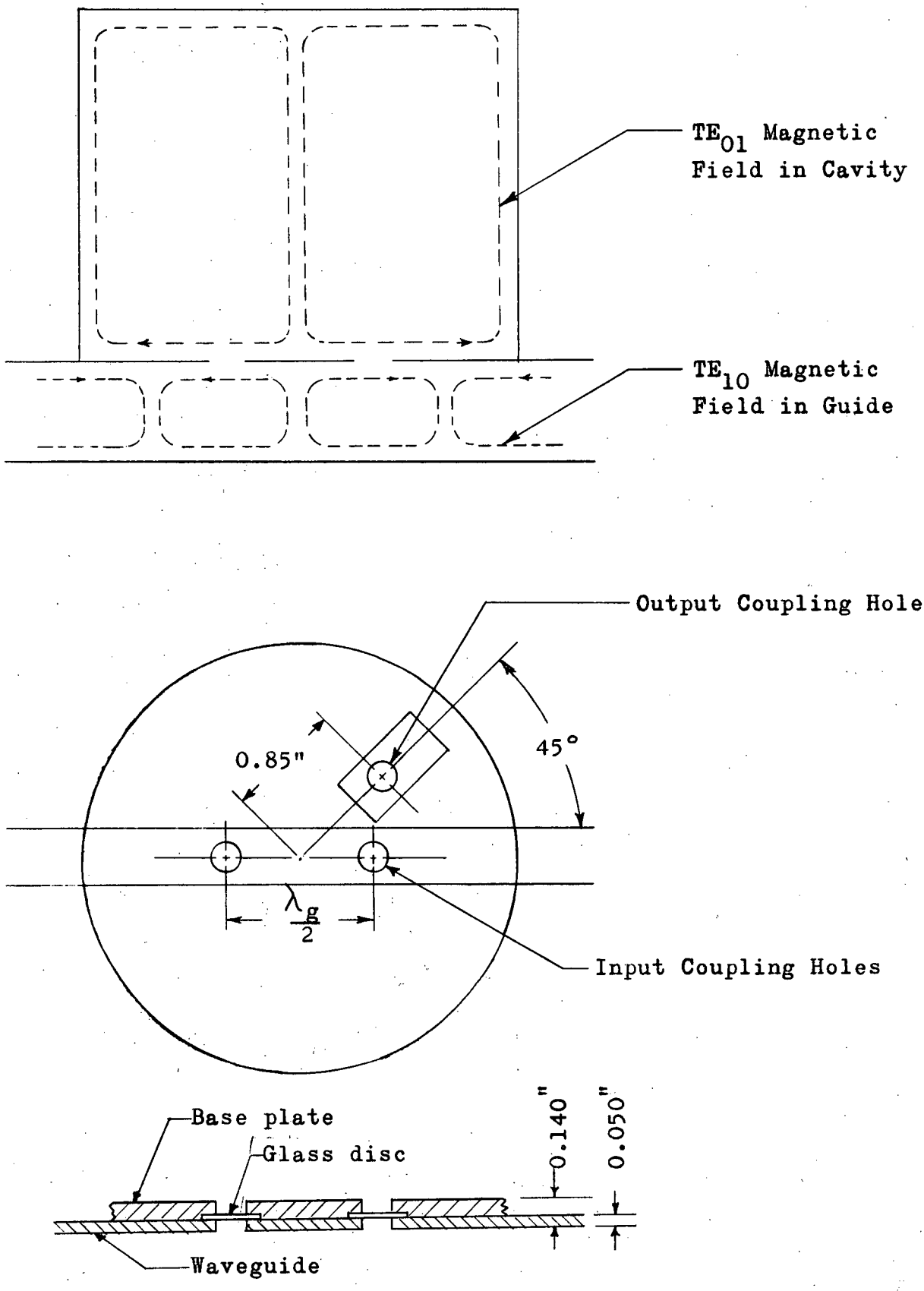

Fig. 2.4 Coupling Configuration

Coupling into the cavity is from the narrow side of a rectangular waveguide through two small holes in the base plate. Coupling out of the cavity is through a third hole in the base plate into the end of another section of rectangular waveguide. The size of the coupling holes was experimentally adjusted until sufficient power was available at the output. A hole diameter of 0.25 inches was used. The coupling holes were sealed with thin glass discs glued to the underside of the base plate.

The theory of the coupling configuration is easily understood. The only field component which exists along the narrow side of a rectangular waveguide operating in the TE_{10} mode is the longtitudinal magnetic field. By coupling from this side of the guide through two small holes placed diametrically opposite in the end wall of the cavity, the longtitudinal magnetic field in the guide is coupled to the radial magnetic field in the cavity. From waveguide theory, the radial magnetic field at the end wall of a cylindrical cavity is, (omitting the term, $e^{j\omega t}$):

For TE modes:

$$H_r = C_1 \frac{\beta}{k} J_n'(kr) \cos n\theta \qquad \ldots 2.3a$$

For TM modes:

$$H_r = - jC_2 \frac{\omega\epsilon n}{rk^2} J_n(kr) \sin n\theta \qquad \ldots 2.3b$$

The holes are spaced one-half wavelength apart in the rectangular guide so that the fields at the holes are of equal magnitude and opposite in phase. As a result of the cos $n\theta$

or sin nθ dependence of the H_r components, only TE or TM waves whose order of n is even will be excited in the cavity by fields phased in this manner.

The output coupling hole is located to reduce the number of undesired modes appearing at the output. Again, because of the form of the θ-dependence, modes corresponding to n = 2 will have a zero H_r field at an angle of 45^o to the input waveguide. Such modes should be eliminated from the output by locating the coupling hole as indicated in Figure 2.4. Although the elimination of undesired modes by this means may be of importance if the cavity is used as a wavemeter, it does not help to solve the fundamental problem of mode interference in the cavity. This can be done only by preventing the excitation of undesired resonances. Since the primary application of the cavity is for tan δ measurements, the location of the output coupling hole is of secondary importance.

The effectiveness of the coupling configuration was investigated over a wide frequency band. Within the range, 8.3 to 8.9 Gc/s, the amplitude of the TE_{01} resonances at the output of the air-filled cavity was greater than that of the strongest undesired mode by a factor of about 200. Upon filling the cavity with oil, this factor was reduced to about 30. The TE_{01} resonances could be satisfactorily excited well outside the frequency range stated but the amplitude reduction of other modes was not nearly as good. This is to be expected since the distance separating the input coupling holes corresponds to exactly one-half wavelength only at the design frequency. For other frequencies, the fields at the coupling

holes are no longer in perfect phase opposition and modes whose order of n is odd can be more easily excited in the cavity.

2.5. Measurement of Q_o and Q_L

Following Ginzton[19], the lumped-parameter equivalent circuit of a cavity with two inputs is shown in Figure 2.5 (a). The input and output coupling to the cavity is represented by ideal transformers, self-inductances and resistive components. Assuming that both the generator and load are matched and neglecting the self-inductances of the coupling elements, this circuit may be transformed into the one of Figure 2.5 (b). The input and output coupling coefficients are defined as

$$\beta_1 = n_1^2 \frac{Z_1}{R_s} ; \qquad \beta_2 = n_2^2 \frac{Z_2}{R_s} \qquad \ldots 2.4$$

Z_1 and Z_2 are the characteristic impedances of the input and output waveguides and the equivalent generator voltage E is equal to $n_1 E_1$.

The unloaded Q of the cavity is

$$Q_o = \frac{\omega_o L}{R_s} .$$

The loaded Q of the cavity is

$$Q_L = \frac{\omega_o L}{R_s + \beta_1 R_s + \beta_2 R_s} \quad \text{or,}$$

$$Q_L = \frac{Q_o}{1 + \beta_1 + \beta_2} \qquad \ldots 2.5$$

The relationship between cavity Q and the transmission resonance curve is obtained as follows:

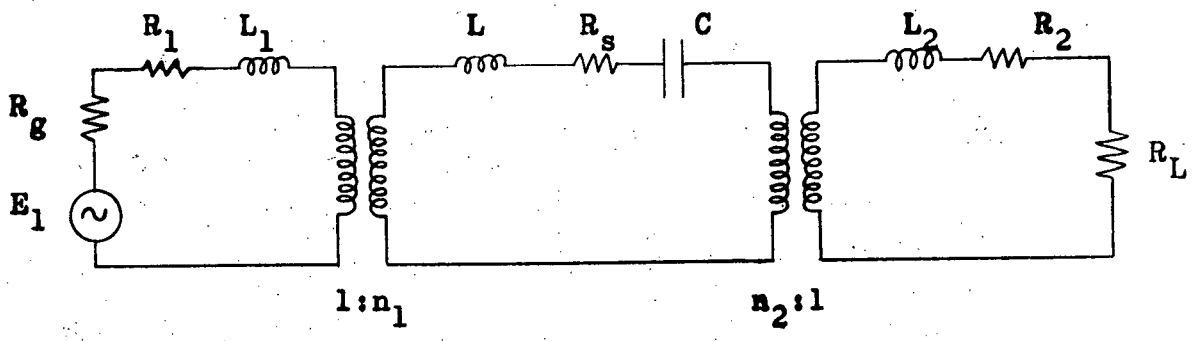

(a)

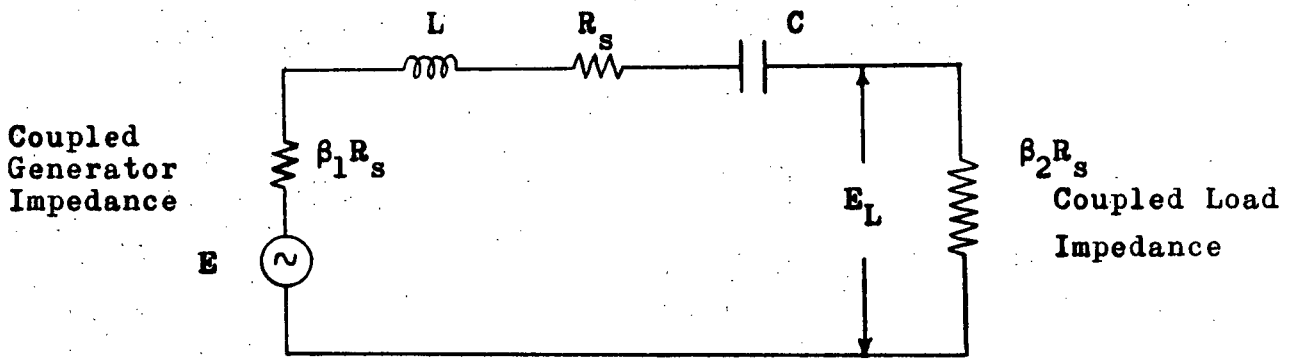

(b)

Fig. 2.5 Lumped-Parameter Equivalent Circuit of the Cavity

The transmission loss $T(\omega)$ is defined as

$$T(\omega) = \frac{P_L}{P_o} \qquad \ldots 2.6$$

where

P_o = Maximum available power from the generator delivered to a matched load.

P_L = Actual power delivered to the load.

Calculating $T(\omega)$ for the equivalent circuit of the cavity,

$$T(\omega) = \frac{4\beta_1\beta_2}{(1 + \beta_1 + \beta_2)^2 + 4\Delta^2 Q_o^2} \qquad \ldots 2.7$$

In this expression, Δ is defined as the tuning parameter;

$$\Delta = \frac{f - f_o}{f_o} = \frac{f_1}{f_o} \qquad \ldots 2.8$$

where f_o is the resonant frequency of the cavity

and f_1 is the deviation from the resonant frequency.

At resonance, $\Delta = 0$. Therefore

$$T(\omega_o) = \frac{4\beta_1\beta_2}{(1 + \beta_1 + \beta_2)^2}$$

and using Equation 2.5 yields the normalized transmission equation:

$$\frac{T(\omega)}{T(\omega_o)} = \frac{1}{1 + 4\Delta^2 Q_L^2} \qquad \ldots 2.9$$

The transmission half-power points occur when $2\Delta Q_L = 1$, from which it follows that

$$Q_L = \frac{f_o}{2f_1} \qquad \ldots 2.10$$

$$Q_o = \frac{f_o}{2f_1}(1 + \beta_1 + \beta_2) \qquad \ldots 2.11$$

This shows that Q_o cannot be calculated directly from the

transmission resonance curve. A separate experiment to measure the coupling coefficients is required. For the case of very loose coupling, β_1 and β_2 are small compared with unity and may be neglected. If this approximation is valid, $Q_o \cong Q_L$ for the empty cavity.

The input coupling coefficient β_1 can be determined from a measurement of the power flow into the cavity at resonance. This measurement is most easily made by removing the matched-load termination on the waveguide run and replacing it with a good short-circuit located to give field maxima at the input coupling holes. A standing-wave detector placed immediately before the cavity in the waveguide run is used to probe the VSWR pattern in the guide. As outlined by Ginzton[20], β_1 can be calculated from the values of VSWR measured for the cases of the tuned and detuned cavity. Measurements of β_1 were made for the empty, partially filled and the completely filled cavity. In each case, β_1 was found to be approximately equal to 0.01. The output coupling coefficient β_2 cannot be measured but it is assumed to be of the same order as β_1. On the basis of these measurements, the loose-coupling approximation was taken as being valid.

The Q_o values of the first three TE_{01} resonances were measured and compared with the theoretical Q_o values. The results are listed in Table 2.1.

In calculating the theoretical Q_o, a skin depth of 1.48×10^{-4} cm for brass has been used. The first two resonances indicate that, due to surface roughness, the effective skin depth was approximately 10 percent greater than

the theoretical value. The additional reduction in measured Q_o for the third resonance is probably a result of the cavity being constructed in two sections. The second section is used to lengthen the cavity so that the TE_{013} resonance can be located. An imperfect junction between the two sections would increase the wall losses in this area and probably is the reason for the reduced Q_o observed.

Table 2.1. Q_o Values

Resonance	Theoretical Q_o	Experimental Q_o	Ratio of Exper./Theor. Q_o Values
TE_{011}	9,340	8,250	0.883
TE_{012}	16,850	15,000	0.891
TE_{013}	28,300	21,000	0.75

2.6. Initial Tests with the Filled Cavity

Several difficulties were encountered in attempting to make tan δ measurements with a cavity completely filled with oil. For the purpose of Q measurement, a signal-to-noise ratio of 25:1 was desirable. This permitted measurements to be made with ease but required a resonance curve amplitude of not less than 200 microvolts at the detector output. Signals of this amplitude could be obtained for the lower-loss samples tested but the higher-loss specimens gave an output about an order of magnitude below this level.

A second problem involved the frequency modulation

characteristics of the reflex klystron. In order to obtain maximum power from the klystron, it was operated near its absolute maximum ratings. Under these conditions the electrical tuning available was 20 Mc/s of which only a central portion 1 Mc/s in width was free from amplitude modulation. For small deviations from the centre frequency, the power output of the klystron decreased symmetrically about f_o and had dropped off 0.8 db at a deviation of 4 Mc/s. For larger deviations, the decrease in output power was more rapid and was no longer symmetrical about the centre frequency.

A further complication was discovered upon investigation of the output detector response as a function of frequency. Two different detector heads and matching units were employed but no combination of these permitted the detector to be broad-banded sufficiently to give a frequency independent response over the swept-frequency band of the klystron. The optimum adjustment of the matching unit was a compromise between output amplitude and detector bandwidth and yielded a response which was down only slightly at a deviation of 4 Mc/s.

Due to the klystron modulation characteristics and the detector response, only the central portion of the klystron tuning mode could be used. For the symmetrical part of the klystron power-output curve, a correction for amplitude modulation can be derived very easily. Therefore it was decided to limit the width of the resonance curve so that the half-power points fell within 4 Mc/s of the centre frequency. In accordance with this restriction, the minimum value of loaded Q which could be measured was approximately 1000.

Completely filling the cavity with the oils tested in later experiments resulted in a loaded Q considerably below this value. As a result, it was necessary to use a cavity only partly filled with oil for the tan δ measurements. This automatically provided adequate power at the detector output but introduced some additional mode-interference problems which are discussed in a later section.

2.7. Fields in the Cavity

From waveguide theory, the fields in a cylindrical resonant cavity are given by [21], (omitting the term, $e^{j\omega t}$):

For TE Modes:

$$E_z = 0$$

$$H_z = J_n(kr) \cos n\theta \sin \beta z$$

$$H_r = \frac{\beta}{k} J_n'(kr) \cos n\theta \cos \beta z \qquad \ldots 2.12a$$

$$H_\theta = - \beta \frac{n}{rk^2} J_n(kr) \sin n\theta \cos \beta z$$

$$E_r = j\omega\mu \frac{n}{rk^2} J_n(kr) \sin n\theta \sin \beta z$$

$$E_\theta = j \frac{\omega\mu}{k} J_n'(kr) \cos n\theta \sin \beta z$$

For TM Modes:

$$H_z = 0$$

$$E_z = J_n(kr) \cos n\theta \cos \beta z$$

$$E_r = - \frac{\beta}{k} J_n'(kr) \cos n\theta \sin \beta z$$

$$E_\theta = \beta \frac{n}{rk^2} J_n(kr) \sin n\theta \sin \beta z \qquad \ldots 2.12b$$

$$H_r = - j \frac{\omega \epsilon n}{rk^2} J_n(kr) \sin n\theta \cos \beta z$$

$$H_\theta = - j \frac{\omega \epsilon}{k} J_n'(kr) \cos n\theta \cos \beta z$$

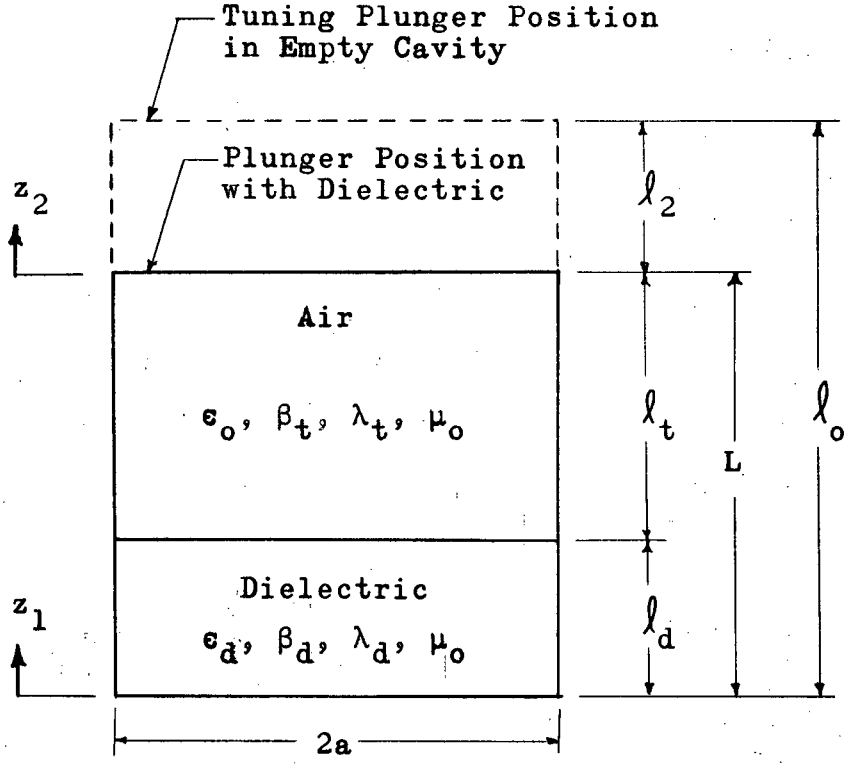

Figure 2.6 Schematic of Cavity

A cylindrical cavity designed to resonate in the TE_{01} mode and partially filled with dielectric is illustrated in Figure 2.6. At resonance, TE_{01} waves exist in each section of the cavity. From Equation 2.12a, the field equations for this mode are written as:

In the air-filled portion:

$$H_z = C_t \, J_o(kr) \sin \beta_t z_2$$

$$H_r = C_t \frac{\beta_t}{k} J_o'(kr) \cos \beta_t z_2 \qquad \ldots 2.13a$$

$$E_\theta = jC_t \frac{\omega \mu_o}{k} J_o'(kr) \sin \beta_t z_2$$

In the dielectric-filled portion:

$$H_z = C_d \, J_o(kr) \sin \beta_d z_1$$

$$H_r = C_d \frac{\beta_d}{k} J_o'(kr) \cos \beta_d z_1 \qquad \ldots 2.13b$$

$$E_\theta = jC_d \frac{\omega \mu_o}{k} J_o'(kr) \sin \beta_d z_1$$

In these equations, C_t and C_d are constants which allow for the possibility of waves of different amplitudes in the two sections.

The boundary conditions to be satisfied at the air-dielectric interface are that the following field components be continuous:

(a) The tangential component of the magnetic intensity H,

(b) The tangential component of the electric field E,

(c) The normal component of the magnetic induction B,

(d) The normal component of the electric displacement D.

Applying the boundary conditions at $z_1 = \ell_d$, $z_2 = -\ell_t$, two equations are obtained:

$$C_d \sin \beta_d \ell_d = - C_t \sin \beta_t \ell_t \qquad \ldots 2.14$$

$$C_d\beta_d \cos \beta_d \ell_d = C_t\beta_t \cos \beta_t \ell_t \quad \ldots 2.15$$

Dividing these two equations yields the resultant equation which must be satisfied for a TE_{01} resonance to exist in the partly filled cavity:

$$\frac{1}{\beta_d} \tan \beta_d \ell_d = -\frac{1}{\beta_t} \tan \beta_t \ell_t \quad \ldots 2.16$$

Equation 2.16 may be put in a different form by using the relation $\ell_t = \ell_o - (\ell_d + \ell_2)$, where

ℓ_o = resonant length of the empty cavity,

ℓ_2 = reduction in resonant length due to the addition of the dielectric.

Since ℓ_o corresponds to an integral number of half wavelengths $\frac{\lambda_t}{2}$, and $\beta_t = \frac{2\pi}{\lambda_t}$, it follows that $\tan \beta_t \ell_o = 0$ and Equation 2.16 becomes

$$\frac{1}{\beta_d \ell_d} \tan \beta_d \ell_d = \frac{1}{\beta_t \ell_d} \tan \beta_t (\ell_d + \ell_2) \quad \ldots 2.17$$

The right-hand side of this equation is known in terms of the measured quantities ℓ_2, ℓ_d and λ_t. Thus, λ_d may be calculated by solving an equation of the form $\frac{\tan \phi}{\phi} = A$, where $\phi = \frac{2\pi}{\lambda_d} \ell_d$. Having obtained λ_d, the dielectric constant ϵ_r may be evaluated by using Equation 2.1 in the form

$$\epsilon_r = \lambda_o^2 \left(\frac{1}{\lambda_d^2} + \frac{1}{\lambda_c^2}\right) \quad \ldots 2.18$$

2.8. Expression for Tan δ

The Q of a resonant cavity is defined as

$$Q = \omega \frac{\text{Total Stored Energy}}{\text{Average Power Loss}} \quad \ldots 2.19$$

For a resonator partly filled with dielectric, this expression is written as

$$Q = \omega \frac{U_t + U_d}{P_w + P_d} \qquad \ldots 2.20$$

where U_t is the energy stored in the air portion, U_d is the energy stored in the dielectric portion, P_w is the average power loss on the walls and P_d is the average power loss in the dielectric.

The quality factor of the dielectric alone is defined as

$$Q_d = \omega \frac{U_d}{P_d} = \frac{1}{\tan \delta} .$$

Hence, the loss tangent of the dielectric may be derived from the measured Q of the partly filled cavity by rearranging the terms of Equation 2.20:

$$\tan \delta = \frac{1}{Q} \left[\frac{U_t}{U_d} + 1 \right] - \frac{P_w}{\omega U_d} \qquad \ldots 2.21$$

The stored energies and power losses on the walls are calculated from the field components in the cavity assuming the fields to be those which would occur for the case of a loss-free dielectric. The calculations are simplified considerably by choosing the depth of dielectric l_d to correspond to an integral number of half wavelengths in the dielectric so that a node of the transverse E-field occurs at the air-dielectric interface. It can easily be shown that for this field distribution, the mean magnetic stored energy equals the mean electric stored energy in each of the air and dielectric-filled portions, thus enabling the stored energies to be determined from either the magnetic or electric field alone. Choosing the simpler form,

$$U_t = \frac{1}{2} \epsilon_o \int_{\text{Air Volume}} |E|^2 \, dv \qquad \ldots 2.22$$

$$U_d = \frac{1}{2} \epsilon_d \int_{\text{Dielectric Volume}} |E|^2 \, dv \qquad \ldots 2.23$$

An approximation for the wall losses may be obtained by assuming the wall to have a uniform conductivity of effective value σ_e. This determines an effective skin depth Δ_e. From a consideration of the Poynting vector at the wall surface, the power flow into the wall is written as an integral[22]:

$$P_w = \frac{1}{2 \Delta_e \sigma_e} \int_{\text{Wall Area}} |H_T|^2 \, ds \qquad \ldots 2.24$$

where H_T is the tangential component of the magnetic field at the wall surface. The product $\Delta_e \sigma_e$ is expressible as a function of Q_o, the experimentally measured value of unloaded cavity Q. This provides a means of eliminating this product from Equation 2.24.

Evaluation of the stored energies and wall losses has been carried out in the Appendix. Substituting these values into Equation 2.21 yields the result:

$$\tan \delta = \frac{1}{Q} \left[1 + \frac{n_2}{n_1 \epsilon_r} \frac{\lambda_t^3}{\lambda_d^3} \right] - \frac{1}{n_1 \epsilon_r Q_o} \left\{ \frac{n_2 \frac{\lambda_t^3}{\lambda_d^3} + 4a \frac{\lambda_c^2}{\lambda_d^3} + n_1}{1 + \frac{4a}{\nu} \frac{\lambda_c^2}{\lambda_t^3}} \right\} \qquad \ldots 2.25$$

where,

Q = the measured loaded Q of the partly filled cavity,

n_1 = the number of half wavelengths in the dielectric,

n_2 = the number of half wavelengths in the air portion,

Q_o = the measured Q of the empty cavity,

ν = the number of half wavelengths in the empty cavity when Q_o was measured,

ϵ_r = the dielectric constant of the dielectric.

Except for a slightly different notation of n_1 and n_2, Equation 2.25 is the result quoted by Penrose[23].

Although a general expression for tan δ which is valid for an arbitrary depth of dielectric may be derived, there are important reasons for choosing ℓ_d to be an integral number of half wavelengths so that the E-field is zero at the air-dielectric interface:

(a) Since the losses in the dielectric are a minimum where the electric field is a minimum, the interface region makes only a small contribution to the measured loss tangent. Therefore, small errors in the dimension ℓ_d or poor levelling of the cavity will have only very minor effects on the accuracy of the measurement.

(b) Meniscus effects are negligible.

(c) Small changes in ℓ_d do not detune the cavity. This prevents mechanical vibrations which perturb the liquid surface from causing instability of the resonance curve displayed on the oscilloscope. This point is quite important experimentally.

The fact that small changes in ℓ_d do not detune the cavity can be shown very easily. If L is the total length of the partly filled cavity at resonance, differentiating Equation 2.16 shows that $\frac{dL}{d\ell_d} = 0$ for $\ell_d = n_1 \frac{\lambda_d}{2}$.

2.9. Preliminary Tests with the Partially Filled Cavity

A series of tests were carried out to determine how well the theoretical expectations were borne out experimentally for a commercial transformer oil. A test frequency of 8.71 Gc/s was selected because the operation of the klystron was most satisfactory at this frequency. The first experiment had three main objectives:

(a) To investigate how accurately λ_d and ϵ_r could be measured with the partly filled cavity,

(b) To determine how significant small errors in ℓ_d and levelling of the cavity are when measuring tan δ,

(c) To eliminate any mode interference which might be present.

The value of λ_t was first determined directly by measuring the distance between the resonances in the air-filled cavity. In a similar manner, λ_d was obtained directly by measuring the distance between resonances when the cavity was completely filled with oil. Using Equation 2.18, an accurate value of ϵ_r is obtained. As discussed previously, the resonance curve produced by the filled cavity is too broad for Q measurement but is suitable for determining λ_d and ϵ_r with an error of about one part per thousand.

In order to investigate how accurately λ_d and ϵ_r could be measured with the partly filled cavity, various depths of oil were placed in the cavity and Equation 2.17 was used to calculate values of λ_d and ϵ_r from the measurements corresponding

to each depth. The results are given in Table 2.2. For small oil depths, the calculated values of λ_d and ϵ_r contain large errors, presumably due to the perturbing effects of the coupling holes. For dielectric depths of approximately one-half wavelength, the values obtained with the partly filled cavity are essentially the same as those measured with the completely filled cavity. Subsequent experiments confirmed that λ_d and ϵ_r could be measured satisfactorily with the partly filled cavity provided the oil depth was approximately one-half wavelength.

Table 2.2. Initial Measurements of λ_d and ϵ_r

Oil Quantity ml	Oil Depth inches	Calculated λ_d inches	Calculated ϵ_r inches
10.0	0.0814	1.067	1.905
20.0	0.1628	1.030	2.025
30.0	0.2442	1.013	2.085
40.0	0.3255	1.005	2.110
50.0	0.4069	0.998	2.135
60.0	0.4883	0.994	2.150
65.0	0.5290	0.994	2.150
70.0	0.5697	0.995	2.145

Test Frequency = 8.71 Gc/s

λ_d measured with the filled cavity = 0.9940 inches

ϵ_r measured with the filled cavity = 2.150 inches

Measured λ_t = 1.6030 inches

Theoretical λ_t = 1.604 inches

The measured Q was expected to remain constant for small changes in ℓ_d from the half-wavelength value. The tuning plunger could be adjusted so that the resonance curve displayed on the oscilloscope corresponded to either the TE_{012} or TE_{013} resonance. Contrary to expectations, it was found that mode interference was present and caused the Q of both resonances to change quite drastically as ℓ_d was varied slightly. An attempt to remove the interference by changing the frequency of the klystron oscillator by a few Mc/s was not successful.

A new frequency of 8.825 Gc/s appeared at first to be satisfactory. In order to investigate more systematically the effects of varying ℓ_d, a calibrated pipette was mounted as a burette and connected to the drain in the base plate of the cavity. This allowed the oil depth to be varied continuously in a known manner while the resonance curve was being observed on the oscilloscope. Graphs illustrating the mode interference encountered are given in Figure 2.7. For purposes of curve comparison, the Q-factors of the two resonances have been normalized.

It is significant to note that the curve shapes are very similar, a fact which indicates the interfering mode is not influenced by plunger travel in the air section of the cavity. At a given frequency, the presence or absence of an interfering mode appeared to be determined solely by the depth of oil present. This type of interference would not be caused by normal resonances whose waves are propagating in both sections of the cavity. However, ghost-mode resonances, consisting of propagating waves in the dielectric section and evanescent

waves in the air section, could cause such interference. These resonances do not tune with the plunger if it is far enough away from the liquid surface. It was temporarily assumed and later confirmed that the troublesome interfering modes were of the ghost-mode variety.

In view of the severe mode interference in the vicinity of the correct depth in Figure 2.7, a systematic search for a more suitable frequency was made in the band 8.3 to 8.9 Gc/s. Between 8.3 and 8.4 Gc/s, there was no interference observed for oil depths near the half-wavelength value. The frequency of 8.395 Gc/s was finally selected and used for all of the later tests. The graphs of Figure 2.8, obtained in the same way as those of Figure 2.7, illustrate the amount of error in l_d permitted before the measured Q-factor is affected.

There were no errors due to mode interference detectable in any of the actual tests performed later. It was also confirmed that levelling the cavity approximately by a visual inspection was perfectly adequate provided the oil depth was near the half-wavelength value. An accurate levelling did not produce any measureable change in Q. The effects of mechanical vibrations caused by the various cooling motors in the power supplies were completely negligible.

2.10. Ghost-Mode Resonances

From Equation 2.1 it follows that waves which are propagating in the dielectric region and evanescent in the air region can occur for any mode whose cut-off wavelength lies in the range such that

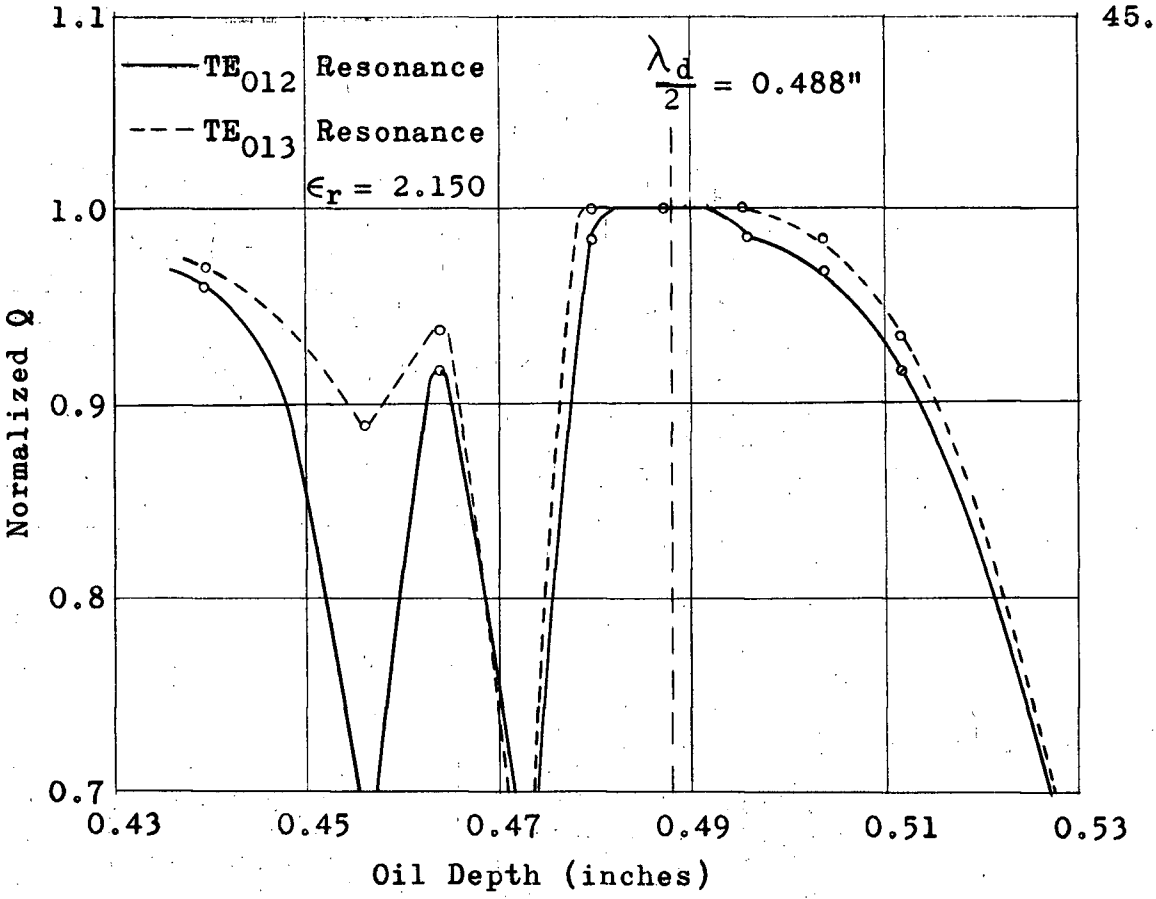

Fig 2.7 Normalized Q versus Oil Depth at 8.825 Gc/s

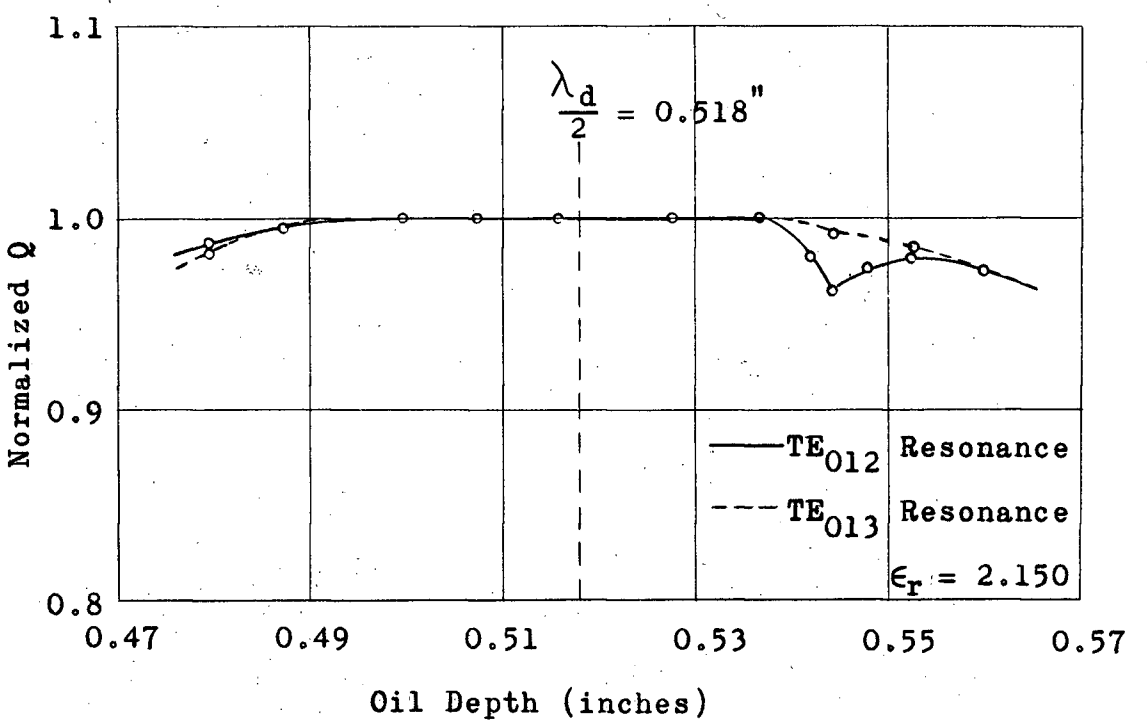

Fig. 2.8 Normalized Q versus Oil Depth at 8.395 Gc/s

$$\frac{\epsilon_r}{\lambda_o^2} > \frac{1}{\lambda_c^2} > \frac{1}{\lambda_o^2} .$$

For these modes, the propagation constant in the air region, $j\beta_t$, is real and positive defining the attenuation constant

$$\alpha = 2\pi \left[\frac{1}{\lambda_c^2} - \frac{1}{\lambda_o^2} \right]^{1/2} \qquad \ldots 2.26$$

The evanescent waves have a longtitudinal dependence described by hyperbolic functions rather than by trigonometric functions. For the air region, the following substitutions are made:

$$\begin{aligned} j\beta_t &= \alpha \\ \sin \beta_t \ell_t &= - j \sinh \alpha \ell_t \qquad \ldots 2.27 \\ \cos \beta_t \ell_t &= \cosh \alpha \ell_t \end{aligned}$$

These substitutions, when applied to Equation 2.16, yield the conditional equation which must be satisfied for a TE ghost-mode resonance to be excited. Although Equation 2.16 was derived for the specific case of the TE_{01} resonance, it clearly applies to all TE resonances in the partly filled cavity. Hence, the condition for any TE ghost-mode resonance to occur is given by

$$\tan \beta_d \ell_d = - \frac{\beta_d}{\alpha} \tanh \alpha \ell_t \qquad \ldots 2.28$$

The matching condition for an arbitrary TM mode can be derived in an identical manner starting from the appropriate field equations given by Equation 2.12b. The result is:

$$\beta_d \tan \beta_d \ell_d = - \epsilon_r \beta_t \tan \beta_t \ell_t \qquad \ldots 2.29$$

For a TM ghost-mode resonance, this becomes

$$\tan \beta_d \ell_d = \frac{\epsilon_r \alpha}{\beta_d} \tanh \alpha \ell_t \qquad \ldots 2.30$$

The value of the product $\alpha \ell_t$, encountered for the various ghost modes, was generally larger than 2.5. Therefore $\tanh \alpha \ell_t$ is approximately equal to unity and Equation 2.28 and Equation 2.30 take the following simplified forms[24]:

For TE ghost modes:

$$\tan \beta_d \ell_d = - \frac{\beta_d}{\alpha} \qquad \ldots 2.31$$

For TM ghost modes:

$$\tan \beta_d \ell_d = \epsilon_r \frac{\alpha}{\beta_d} \qquad \ldots 2.32$$

The curves of Figure 2.9 have been plotted from these equations and show the theoretical depth of oil for a ghost mode to be excited at a given frequency. It is of interest to note that the interference discussed previously and illustrated in Figure 2.7 can be attributed to the excitation of the TE_{32}, TM_{32} and probably a combination of the TM_{61} and TE_{13} ghost-mode resonances.

An experiment was performed to investigate how strongly the various ghost modes were excited at 8.395 Gc/s. The results are shown in Table 2.3. Several of the resonances were too weak to be observed directly but these could be detected by noting their effect on the TE_{01} modes. As before, the oil depth was varied continuously while the TE_{01} resonance curve was being observed on the oscilloscope. At the depth corresponding to the excitation of a ghost mode, a distinct broadening of the curve and decrease in amplitude occurred for both TE_{012} and TE_{013} resonances. The TE_{32} ghost mode was much

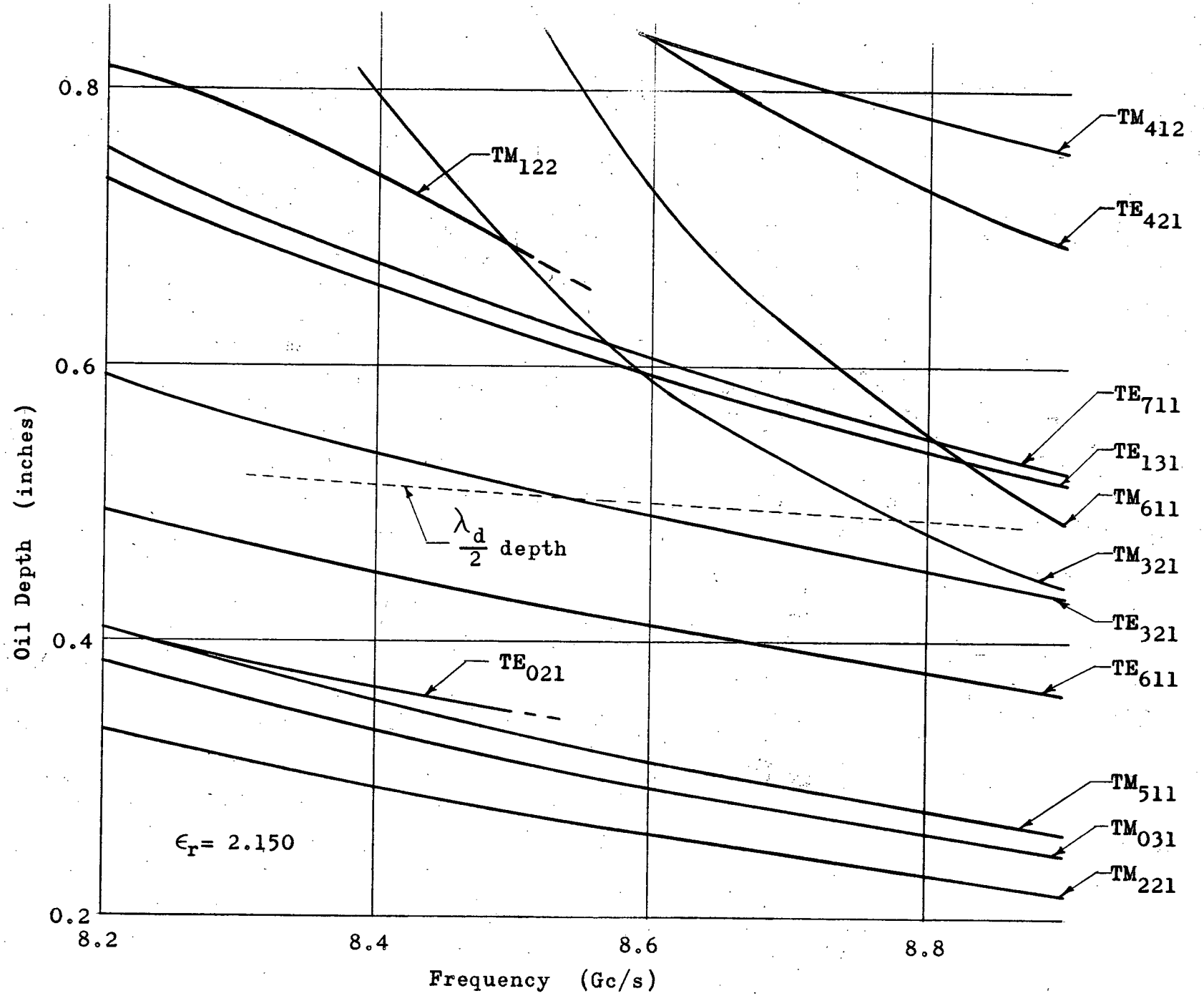

Fig. 2.9 Oil Depth versus Frequency for Ghost Modes

weaker than the others but could still be positively identified. It was also observed that the TE_{02} mode was somewhat tunable with the plunger. This was to be expected since for l_t approximately equal to one inch, putting tanh α l_t equal to unity is not a good approximation.

Table 2.3 Ghost-Mode Resonances

Resonance	Amplitude μ volt	α $inch^{-1}$	Theor. l_d inches	Exper. l_d inches
TM_{221}	100	3.11	0.295	0.295
TM_{031}	*	3.38	0.337	0.341
TM_{511}	25	3.50	0.357	0.361
TE_{021}	50	0.802	0.368	0.384
TE_{611}	*	1.895	0.448	0.456
TE_{321}	*	2.63	0.537	0.545
TE_{131}	*	3.25	0.656	0.659
TE_{711}	*	3.29	0.671	0.676
TM_{122}	*	0.802	0.738	0.741

* Indicates presence detected indirectly

Test Frequency = 8.395 Gc/s

2.11 Propagating Modes in the Cavity

The modes excited in the air-filled cavity were identified by using Equation 2.1 to calculate the theoretical cavity length at which a particular resonance should occur. Table 2.4

lists the resonances excited strongly enough to be observable and compares their approximate actual amplitudes at the detector. Some of the weaker resonances found were due to the excitation of modes in the space behind the tuning plunger rather than in the main portion of the cavity. These could be easily distinguished from the normal ones by noting that since the space behind the plunger is lengthened as the cavity itself is shortened, the tuning behaviour of resonances excited behind the plunger will be reversed.

In a similar manner, Equations 2.16 and 2.29 were used to identify the modes in the partly filled cavity. For the oil depth chosen, the TM_{11} resonances are theoretically degenerate with the TE_{01} resonances but are not excited because of the coupling configuration used. No evidence of interference from the TM_{11} mode could be detected. Other propagating modes in the cavity are sufficiently far removed to eliminate the possibility of interfering with the TE_{01} resonances.

2.12. Correction for Klystron Amplitude Modulation

Amplitude modulation of the klystron causes the frequency separation of the resonance curve half-power points to be less than the true separation which would be measured if the power output of the klystron remained constant over the swept-frequency band. For this reason, the value of Q_L calculated from Equation 2.10 is larger than the true value. An approximate correction for this error will now be derived for that portion of the klystron power-output curve which is nearly symmetrical about the frequency f_o.

Table 2.4 Resonances in the Air-Filled Cavity

Test Frequency 8.395 Gc/s

Mode	Amplitude μ volt	Actual Cav. Length inches	Theor. Cav. Length inches
*	4	0.644	
TE_{111}	30	0.731	0.730
TE_{211}	120	0.787	0.784
TE_{011}	75,000	0.844	0.845
Possibly TM_{111}	40	0.855	0.845
Possibly TE_{311}	10	0.901	0.886
*	20	0.952	
*	10	1.021	
TM_{211}	300	1.059	1.051
TE_{411}	40	1.105	1.102
TE_{121}	200	1.110	1.106
TE_{112}	20	1.460	1.460
TE_{212}	240	1.570	1.568
TE_{012}	70,000	1.688	1.690
*	4	1.708	
Possibly TE_{511}	60	1.872	1.900
or TM_{311}			1.886
TM_{212}	240	2.112	2.103
TE_{113}	10	2.185	2.189
TE_{412}	40	2.206	2.203
TE_{122}	60	2.209	2.212
Possibly TM_{022}	20	2.351	2.340
TE_{213}	200	2.356	2.352
TE_{013}	50,000	2.532	2.534

*Indicates Resonance behind Tuning Plunger

Referring to the equivalent circuit of Figure 2.5(b), the presence of amplitude modulation can be accounted for by assuming the generator voltage to be of the form

$$E = E(f) = E(f_o)\ g(f_1) \qquad \ldots\ 2.33$$

Since the correction is limited to the symmetrical portion of the power-output curve, $g(f_1)$ is an even function describing the frequency dependence of the output in terms of the deviation f_1. With this substitution, the normalized transmission through the cavity becomes

$$\frac{T(\omega)}{T(\omega_o)} = \frac{g^2(f_1)}{1 + 4\Delta^2 Q_L^2} \qquad \ldots\ 2.34$$

The half-power points occur when $\frac{T(\omega)}{T(\omega_o)} = \frac{1}{2}$. Therefore, recalling that $\Delta = \frac{f_1}{f_o}$, the true value of Q_L is calculated from Equation 2.34 and is given by

$$Q_L = \frac{f_o}{2f_1}\left[2g^2(f_1) - 1\right]^{1/2} \qquad \ldots\ 2.35$$

The correction term, $\left[2g^2(f_1) - 1\right]^{1/2}$, can be obtained by using a very simple experimental technique to plot a graph of the function $g^2(f_1)$. At any given frequency, the signal level at the detector is related to the power output of the klystron. Quite generally, the power transmitted through the cavity and delivered to the load represented by the matched detector is

$$P_L(f) = \frac{E_L^2}{\beta_2 R_s} \qquad \ldots\ 2.36$$

Consider the case of the cavity tuned to resonance at a frequency $f = f_o + f_1$. At resonance, the cavity acts as a pure resistance of the value R_s and hence, evaluating E_L, the

power delivered to the load at this frequency is given by

$$P_L(f) = \frac{\beta_2}{(1 + \beta_1 + \beta_2)^2 R_s} \cdot E^2(f_o) g^2(f_1) \qquad \ldots 2.37$$

Similarly, with the cavity tuned to resonance at the frequency f_o, the power delivered to the load at the frequency f_o is

$$P_L(f_o) = \frac{\beta_2}{(1 + \beta_1 + \beta_2)^2 R_s} \cdot E^2(f_o) \qquad \ldots 2.38$$

Dividing these two equations yields the normalized power level at the detector as a function of frequency:

$$\frac{P_L(f)}{P_L(f_o)} = g^2(f_1) \qquad \ldots 2.39$$

In each case the cavity has been tuned to resonance at the frequency in question.

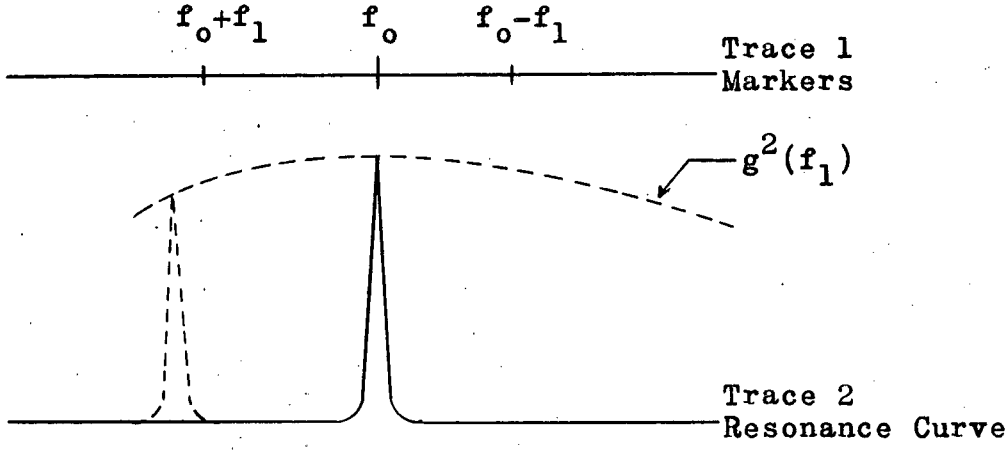

Fig 2.10 Frequency Dependence of Response-Curve Amplitude

From this analysis, it follows that the peak of the resonance curve observed on the oscilloscope traces out the

function $g^2(f_1)$, as the cavity is tuned across the swept-frequency band of the klystron. This is illustrated in Figure 2.10. The cavity is first tuned to the frequency f_o and the amplitude of the resonance curve is noted. The cavity is then tuned to a slightly different frequency $f = f_o + f_1$. The response-curve amplitude will be somewhat lower due to the reduced power output of the klystron at the frequency to which the cavity is tuned. The original level is restored by increasing the power input to the cavity with an adjustment of the precision attenuator. Continuing in this manner, the graph of Figure 2.11 is obtained from the calibration of the precision attenuator. This graph is converted from the decibel scale and is used to produce the required correction curve of Figure 2.12. The correction curve is completely independent of the detector square-law characteristic.

Two assumptions which require some explanation have been made in the foregoing analysis. It has been assumed that the coupling coefficients are independent of frequency and also that the detector stays matched over the frequency range of interest. That β_1 and β_2 do, in fact, remain essentially constant is fairly clear. The fields in the cavity at the end wall are independent of frequency. In the waveguide, the small changes in guide wavelength caused by the frequency deviations from f_o produce completely negligible effects as far as the operation of the coupling holes is concerned.

The matching of the detector is a slightly more difficult problem. Nearly all of the observed decrease in the output level was due to the klystron but a small portion was caused

by the frequency-response characteristic of the detector. The two effects are not easily separated experimentally and the graph of the function $g^2(f_1)$ includes both. However, for purposes of simplicity, the correction has been derived for an ideal detector and $g^2(f_1)$ is assumed to represent the amplitude modulation characteristic of the klystron.

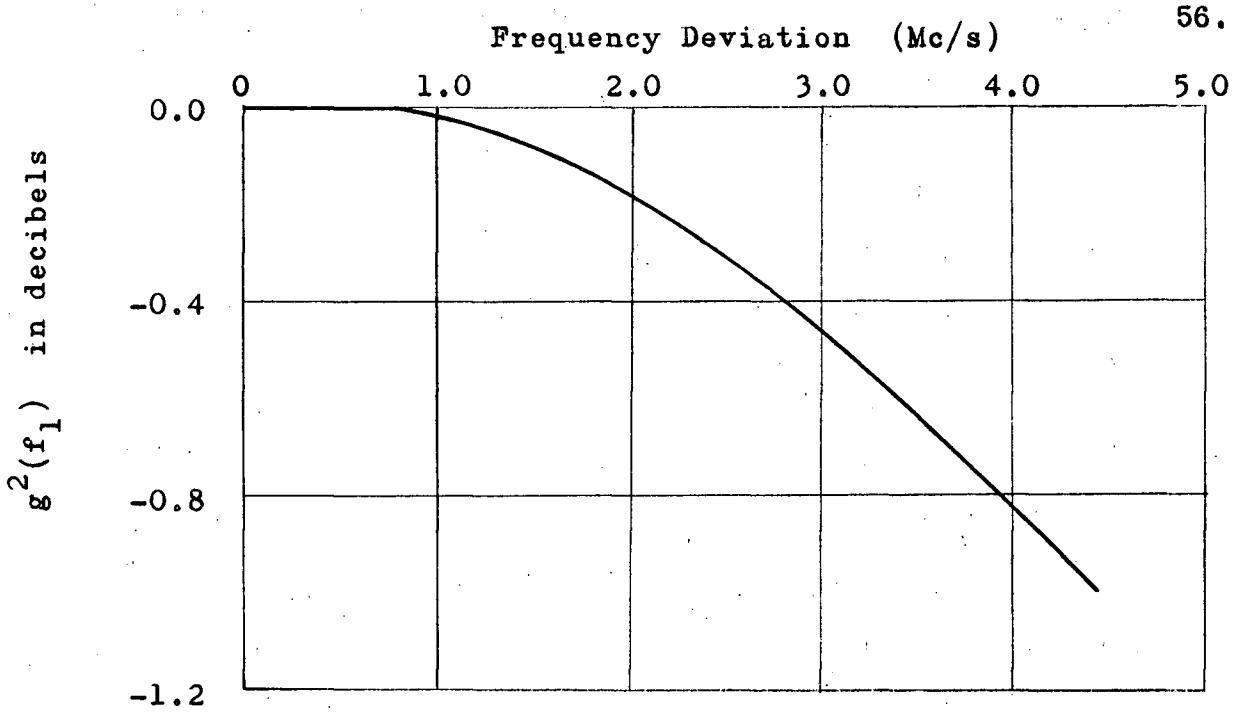

Fig 2.11 Normalized Klystron Power-Output Curve

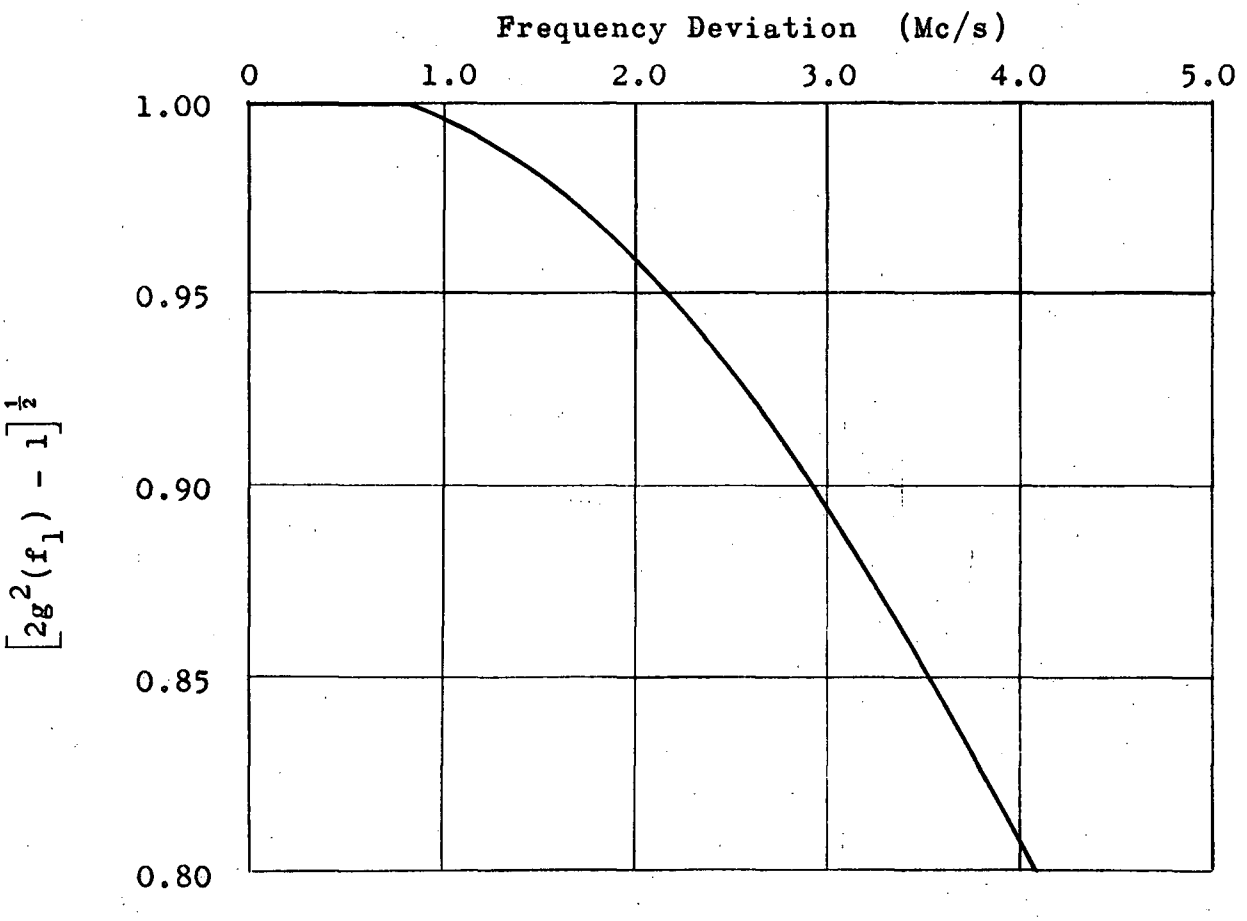

Fig. 2.12 Correction Term

3. TESTS AND RESULTS

3.1. General Procedure

Two transformer oils of commercial quality were selected for the main series of tests. They will be referred to as Oils 1 and 2 and were of the following general types:

Oil 1 - a lightly inhibited oil,

Oil 2 - an uninhibited oil.

These oils were artificially aged by oxidizing them at either 110 or 115 °C. The correlation of tan δ with deterioration was investigated by making tan δ measurements on samples aged different periods of time.

The condition of the aged oils was also determined chemically by evaluating the neutralization number of each sample. Because of the complex and lengthy procedure which is required for a sludge determination, the amount of sludge present in the oxidized oils was inspected visually but was not measured quantitatively.

3.2. Artificially Ageing the Oils

The basic procedure outlined is the one used for the first set of tests. The modifications made prior to a second set of tests are discussed in a following section.

Four oil samples of 120 ml each were put into thoroughly clean, 250-ml Erlenmeyer flasks. The flasks, unstoppered and exposed to the normal room atmosphere, were placed in a thermostatic bath whose temperature was held constant at 110 °C.

An 18-inch length of 12-gauge solid copper wire, carefully cleaned with fine emery and a dry cloth, was coiled in the form of a spiral and placed in the bottom of each flask. This served as a catalyst to speed up the oxidation of the oil. Every 48 hours, one of the samples was removed from the heat bath and allowed to cool to room temperature. Determinations of neutralization number and tan δ were then made.

The heat bath consisted of a well-insulated metal container large enough to accommodate four samples at one time. This container was filled to the proper depth with paraffin and was heated by a hot plate. The temperature of the bath could be adjusted to any value between 80 ^{o}C and 140 ^{o}C. Once adjusted, a simple electronic circuit employing a thermistor immersed in the paraffin, automatically held the temperature constant to within $\pm$ 1 ^{o}C of the set value. The circuit is shown schematically in Figure 3.1.

3.3. Evaluation of Neutralization Number

The neutralization number of the oil was determined following the ASTM Color Titration Method, D974-58T[25]. The method consisted of dissolving a 50-ml oil sample in 100 ml of a titration solvent, adding the indicator and then titrating with a standard alcoholic base solution until the end point was reached. The titration solvent itself was very slightly acidic and required a few drops of base solution for neutralization. A blank titration on 100 ml of the solvent provided a correction for this.

The titration solvent was prepared by adding 5 ml of distilled water and 495 ml of isopropyl alcohol to 500 ml of toluene. The indicator solution was made up by dissolving 2.5 gm of p-naptholbenzein (orange in acid, green-brown in base) in 250 ml of the titration solvent. For each titration, 0.5 ml of this indicator solution was used. The standard base solution was prepared by dissolving 2.5 gm of NaOH in one litre of isopropyl alcohol. This base was standardized frequently by titrating with an aqueous 0.1 N standard HCl solution. The concentration of the base solution was 0.068 N. In order to express the neutralization number in mg KOH per gram, the calculations were done as though KOH had been used in the preparation of the base solution.

3.4. Evaluation of Tan δ

For the measurements of loss tangent, the cavity was filled to a depth corresponding to one-half wavelength in the oil for the TE_{01} mode. Rather than measure the depth of liquid, the filling was done volumetrically with a pipette. The volume of oil required to give the correct depth was calculated from the measured value of ϵ_r and the known diameter of the cavity. For oils which contained sludge, care was taken to ensure that a representative sample was placed in the cavity.

The Q-factors corresponding to the TE_{012} and TE_{013} resonances were measured for each sample. These were corrected for amplitude modulation of the Klystron according to Equation 2.35 and were then substituted into Equation 2.25 to yield the tan δ values.

Equation 2.25 takes a simple form when numerical values are assigned to the various parameters. For example, choosing $\nu = 2$ corresponds to a Q_o value of 15,000 from Table 2.1. This value of Q_o did not change during the entire period that the cavity was used. The radius a is fixed at 1.545 inches, the cut-off wavelength λ_c for the TE_{01} mode is equal to 2.533 inches and the guide wavelength λ_t is equal to 1.688 inches. For Oil 2, ϵ_r is equal to 2.165 and hence, $\lambda_d = 1.032$ inches. All the measurements were made with $n_1 = 1$ and n_2 equal to either 1 or 2. With these substitutions, Equation 2.25 becomes

$$n_2 = 1: \quad \text{Tan } \delta = \frac{3.02}{Q} - 0.000249 \qquad \ldots 3.1$$

$$n_2 = 2: \quad \text{Tan } \delta = \frac{5.04}{Q} - 0.000275 \qquad \ldots 3.2$$

These equations permit tan δ to be calculated from the Q-factor of either the TE_{012} or TE_{013} resonance. For Oil 1, $\epsilon_r = 2.150$ and $\lambda_d = 1.035$ inches. Therefore, a pair of almost identical equations are obtained.

3.5. Test I - Artificially Aged Oils

Samples of Oils 1 and 2 were aged by the method discussed previously. Both oils were clear and bright in appearance and slightly yellow in color at the start of the test. The inhibited oil showed only a slight discoloration and a barely perceptible trace of light grey sludge after 192 hours of ageing at 110 °C. The uninhibited oil darkened rapidly in color and began to produce dark brown sludge when aged for about 36 hours. After 192 hours, the oil was a reddish-brown in color and contained a considerable amount of sludge. Tan δ and acidity measurements

were made on samples aged for various periods of time. The results are given in graphical form in Figure 3.2.

The dielectric constant of the oils was originally measured as 2.150 and 2.165 for Oils 1 and 2 respectively. These values had not changed measureably after ageing the oils in this test.

3.6. Test II - Artificially Aged Oils

It was desirable to make measurements on oils which were more highly oxidized than those of Test I. For this reason, the oils for Test II were oxidized at the higher temperature of 115 ^{o}C. In addition to raising the temperature of the heat bath, the procedure was modified by bubbling filtered air which was dried with silica gel, through each oil sample. This ensured an adequate supply of oxygen for the deterioration process. A sample was removed from the heat bath every 24 hours.

Again, the inhibited oil was deteriorated to a much lower degree than the uninhibited oil. The slight amount of sludge formed by Oil 1 was light grey in color and the oil itself was golden yellow. The aged samples of Oil 2 were very dark in color and were heavily sludged. Tan δ and acidity values are given by the solid-line graphs of Figure 3.3. It was again found that the dielectric constants of the oils had not changed a measureable amount as a result of the ageing process.

A simple test was performed to determine what significance the presence of sludge had on the tan δ and acidity measurements.

The heavily sludged samples of Oil 2, upon which tan δ measurements had already been made, were filtered to remove the sludge. Tan δ and acidity measurements were then made on these filtered oils. The dashed-line graphs of Figure 3.3(b) show the result. The neutralization number of the oil was found to be less after sludge removal but the tan δ value was either the same or slightly increased.

3.7. Test III - Effect of Water

Since water has a polar structure and exhibits a large loss tangent at microwave frequency, the tan δ measured for an oil will be influenced by moisture content. An experiment was performed to determine the magnitude of this effect.

A few drops of distilled water were added to a quantity of Oil 1 in a glass-stoppered flask. This mixture was stored for three weeks until the oil had taken on a cloudy appearance, indicating particles of moisture in suspension. A measurement of tan δ was then made on the oil and was found to have increased from the initial value of 10.8×10^{-4} to 11.8×10^{-4}. No change in dielectric constant was measured.

3.8. Test IV - Oils Removed from Transformers

Three oil samples, removed from transformers in service, were obtained from the Standards Laboratory of the B.C. Hydro and Power Authority. All three of these oils were regarded as worn out and were in the process of being discarded. The loss tangent and dielectric constant values measured for these oils are listed in Table 3.1.

Table 3.1 Measurements on Service-Aged Oils

Sample	Tests by B.C. Hydro Laboratory				Test IV	
	Appearance	ASTM Color	IFT*	N.N.**	Tan δ x 10^4	ϵ_r
Oil 3	Sludge, foggy	2.75	14.5	0.40	35.9	2.150
Oil 4	Sludge, foggy	2.75	13.7	0.76	45.4	2.165
Oil 5				0.98	52.1	2.220

*Interfacial Tension in dynes per cm

**Neutralization Number in mg KOH per gram

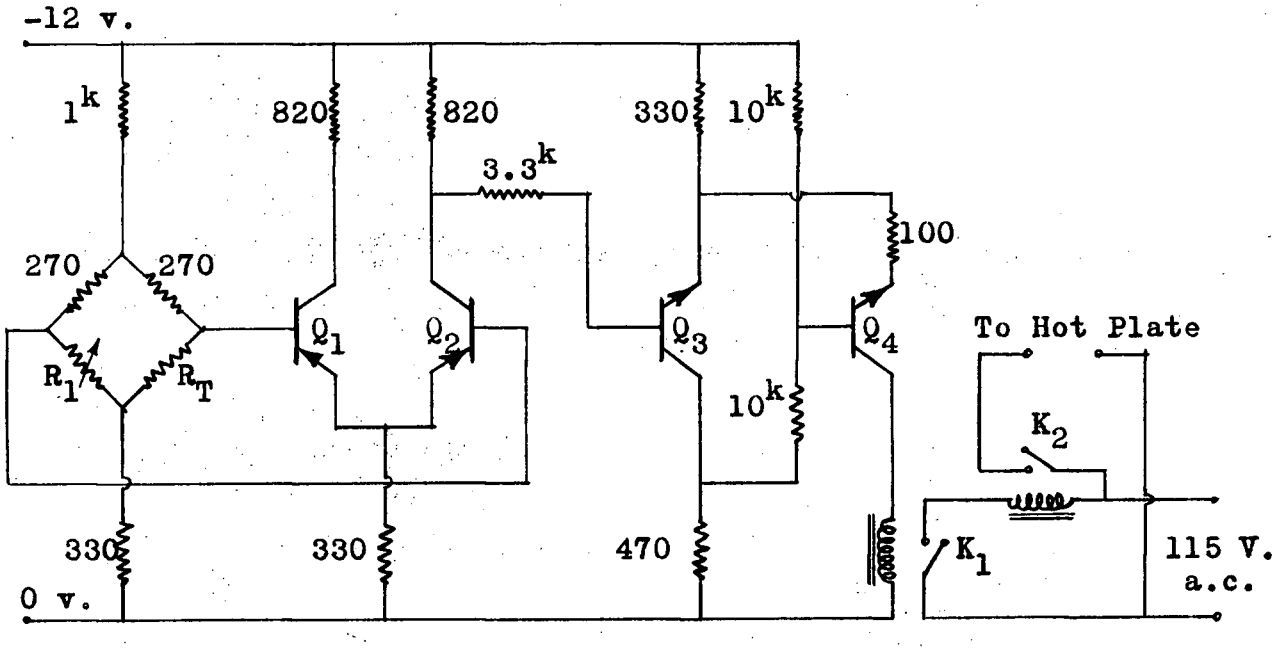

R_1: Decade Box

R_T: GC32A1 Thermistor

Q_1, Q_2: 2N1382 (Selected pair)

Q_3, Q_4: 2N1304

K_1: Magnetic reed Relay

K_2: Power Relay

Fig. 3.1 Temperature Control Circuit

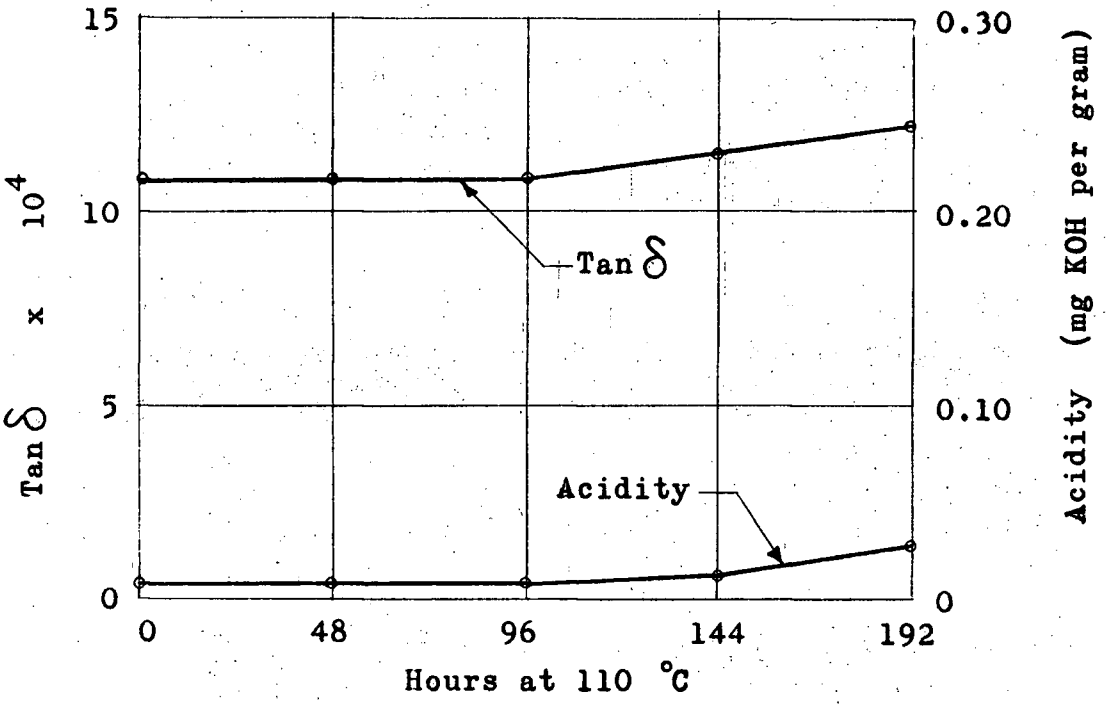

(a) Oil 1

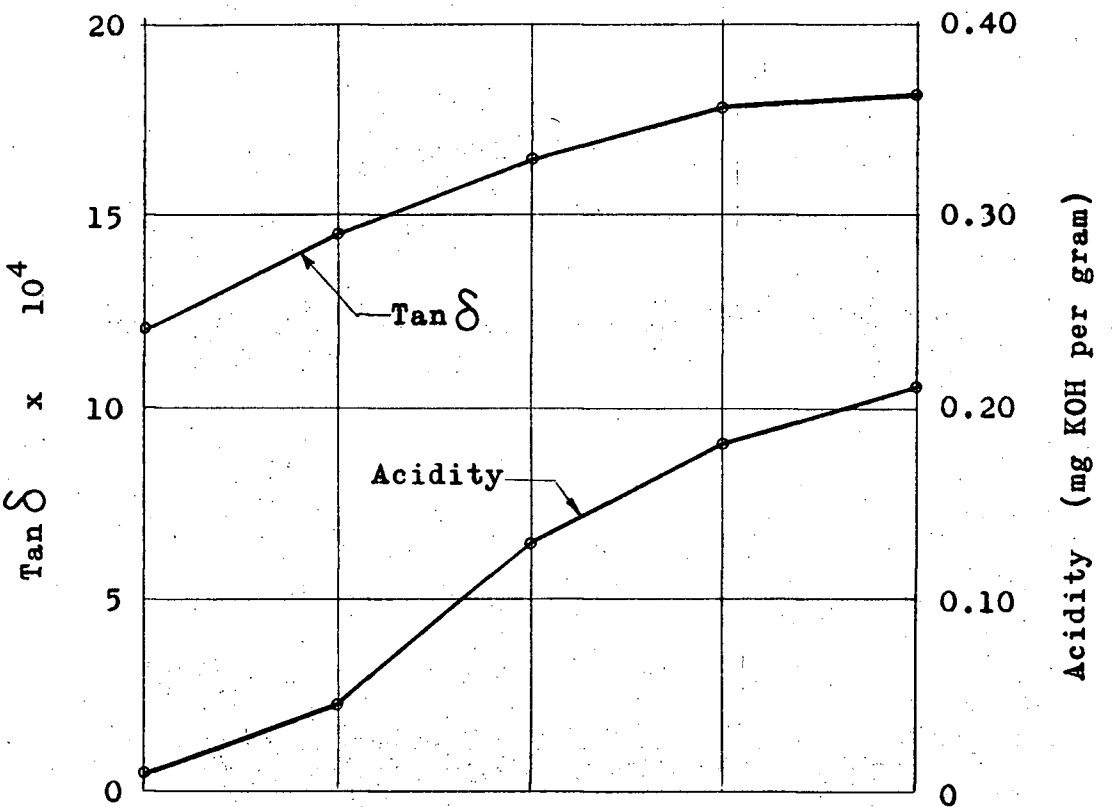

(b) Oil 2

Fig. 3.2 Tan δ and Acidity for Test I

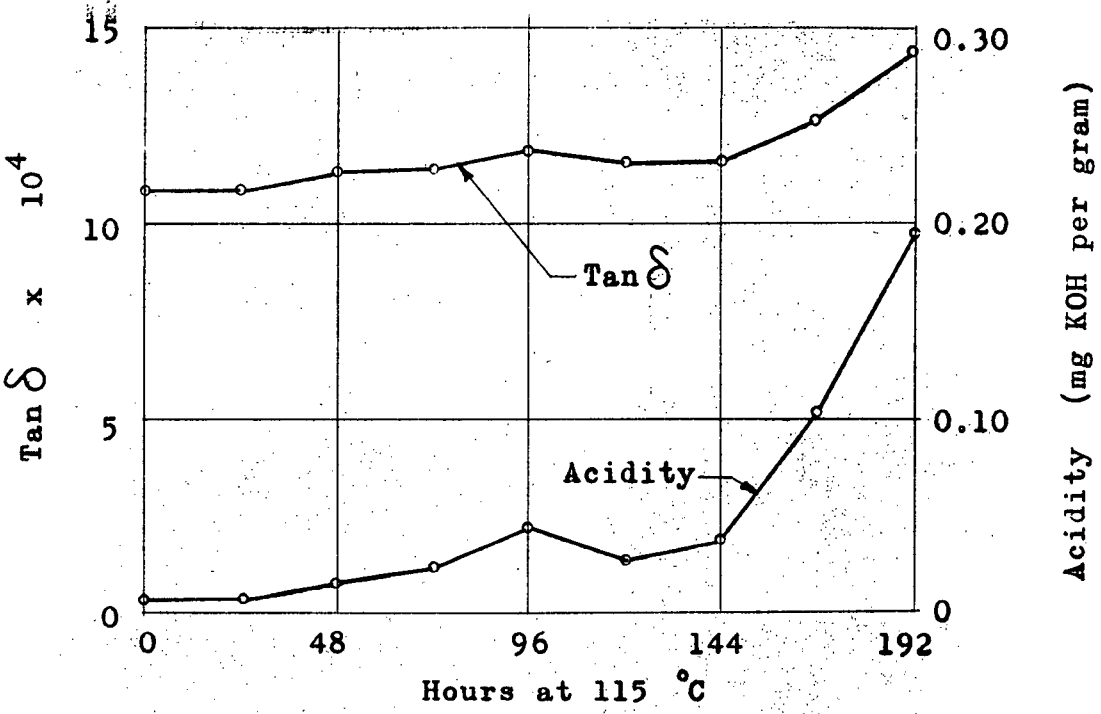

(a) Oil 1

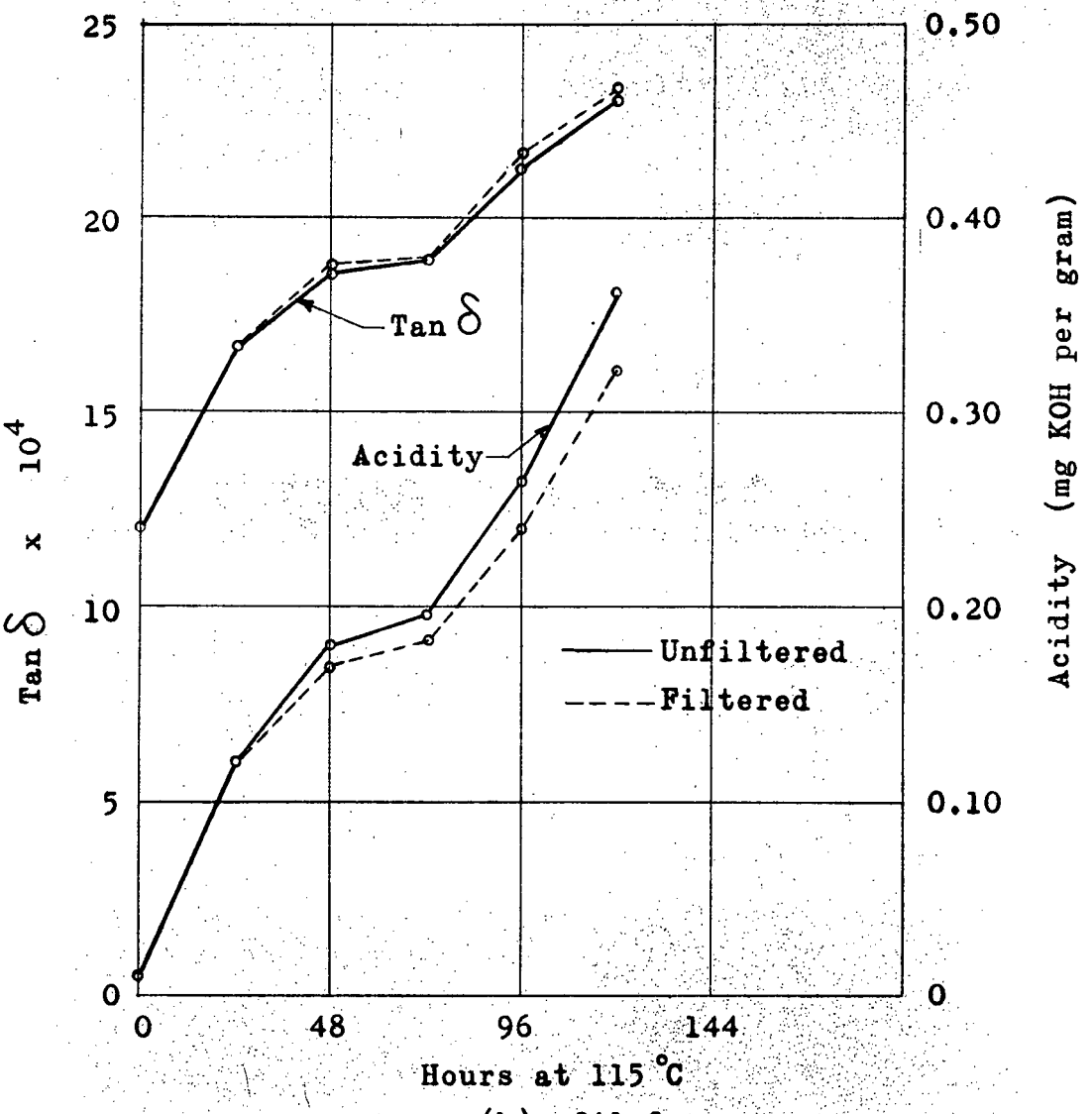

(b) Oil 2

Fig 3.3 Tan δ and Acidity for Test II

3.9. Accuracy of the Measurements

The error contained in the measured tan δ values depends primarily on the following factors:

(a) Calibration error of the precision attenuator,

(b) Random error in measuring the Q-factor of the cavity,

(c) The presence of amplitude modulation in the output of the swept klystron,

(d) The accuracy of Equation 2.25 in correcting for the wall losses in the cavity.

Although the amount of error in tan δ caused by the calibration of the precision attenuator cannot be measured, it is estimated to be less than 1%. For the purpose of Q-measurement, it is required to have two calibration points on the attenuator which correspond to a power difference of exactly 3 db. The absolute amount of attenuation present need not be accurately known. The attenuator used was compared with a rotary-vane attenuator whose absolute accuracy is claimed to be 2% or 0.1 db, whichever is greater. In view of this, the estimate of less than 1% error seems reasonable.

The repeatability of Q measurement was determined by carrying out a number of identical measurements. When measurements on oils were being made, the Q-factors were generally less than 3500 and the repeatability was 1%. For the measurement of unloaded Q-factors in excess of 15,000, oscilloscope trace jitter and broadening of the markers reduced the repeatability to 3%. This uncertainty of 3% in Q_o would not produce an error larger than 0.5% in the value of tan δ.

The errors in tan δ caused by amplitude modulation of the klystron are estimated to be less than 2% after applying the correction described previously. Since tan δ is a constant of the dielectric, Equations 3.1 and 3.2 should yield identical values if there is no amplitude modulation present. In the case when the swept klystron is also amplitude modulated, the value of tan δ calculated from the TE_{012} resonance will be consistently lower than that calculated from the TE_{013} resonance. This is illustrated in Table 3.2 which gives the uncorrected and corrected values of tan δ calculated for the aged samples of Oil 2 in Test II. The corrected values of tan δ differ by less than 2% in all cases.

Table 3.2 Calculated Values of Tan δ for Oil 2

Hours at 115°C	Resonance	f_1 Mc/s	Uncorrected tan δ x 10^4	Corrected tan δ x 10^4
0	TE_{012}	1.93 ± 0.01	11.4	11.9
0	TE_{013}	1.23 ± 0.01	12.0	12.1
24	TE_{012}	2.48 ± 0.02	15.3	16.6
24	TE_{013}	1.59 ± 0.01	16.3	16.8
48	TE_{012}	2.70 ± 0.02	16.9	18.7
48	TE_{013}	1.72 ± 0.01	17.9	18.5
72	TE_{012}	2.72 ± 0.02	17.1	18.9
72	TE_{013}	1.74 ± 0.01	18.1	18.7
96	TE_{012}	2.98 ± 0.03	19.0	21.4
96	TE_{013}	1.92 ± 0.01	20.3	21.2
120	TE_{012}	3.14 ± 0.03	20.1	23.0
120	TE_{013}	2.04 ± 0.02	21.8	22.9

The close agreement of the corrected values of tan δ in Table 3.2 also indicates that the wall losses in the cavity have been properly accounted for. It is not possible to determine exactly the magnitude of the error introduced by the correction for wall losses since it depends on the validity of the assumptions made in deriving Equation 2.25. An estimate of the error limit is obtained by the following reasoning.

The two basic assumptions made in deriving Equation 2.25 were that

(a) Except for a magnitude factor, the fields in the cavity are those which would occur for a loss-free dielectric,

(b) The wall losses can be calculated in terms of a effective wall conductivity σ_e.

The first of these assumptions is in general use and is taken as being valid. The second is also in general use and can be partially justified. A value for σ_e can be calculated from an experimental measurement of Q_o for a particular resonance in the air-filled cavity. Using this value of σ_e, the Q_o of other resonances can then be predicted with an error of less than 10%. Thus, it seems reasonable to use this same value of σ_e when calculating the wall losses in the dielectric-filled cavity. On this basis, since the wall losses were less than 20% of the dielectric losses, the error in tan δ from this source is regarded as being less than 1.5%.

In view of the foregoing sources of error, the absolute error of the measured tan δ values is estimated to be less than 6%. For the purpose of comparing tan δ values of different

samples without regard to the absolute value, the error is less than 2%.

Dielectric constant measurements made with the completely filled cavity have an error of less than 0.1%. Measurements of dielectric constant for the aged samples were made with the cavity partly filled. For these, the error is less than 0.25%.

The repeatability of the acidity measurements can be summarized briefly as follows. The samples of Oil 1 were all lightly colored so that the estimated repeatability is better than 0.01 mg KOH per gram. For the aged samples of Oil 2, the darker color made observation of the end point more difficult and the estimated repeatability is 0.03 mg KOH per gram.

3.10. Discussion of Results

The graphs of Figure 3.2 and 3.3 show that a correlation exists between the measured values of tan δ and acidity for the aged oils. Some of the qualitative aspects of this correlation may be deduced from the graphs of Figure 3.4 which have been prepared by plotting the incremental changes occurring during the ageing experiments. Referring to Figure 3.4, several observations can be made:

(a) The relation between tan δ and acidity is approximately linear except for the very early stages of oxidation,

(b) The increase in loss tangent which occurs is related to the nature of the oil and also to the conditions under which the oxidation takes place,

(c) For the same increase in acidity, the increase in loss tangent for Oil 2 is approximately twice that for Oil 1.

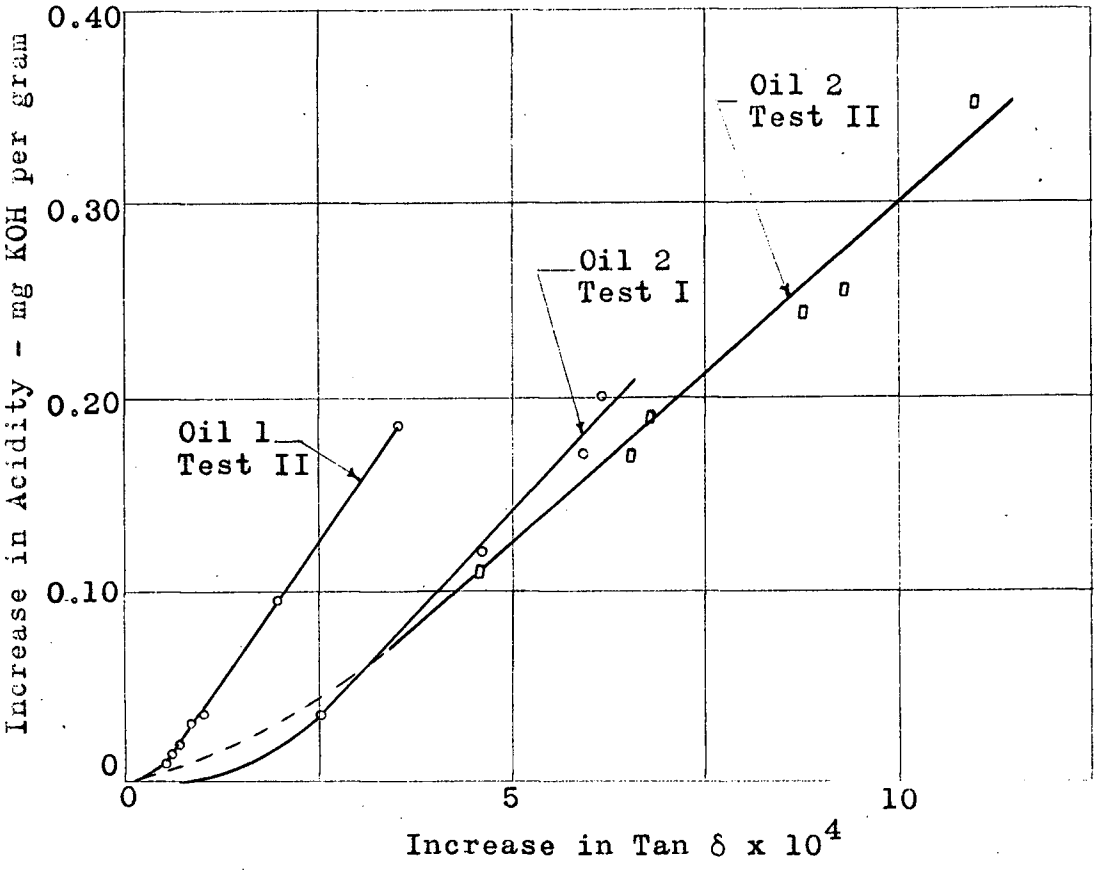

Fig. 3.4 Increase in Acidity versus Increase in Tan δ

Although the correlation between the loss tangent and acidity is very definite, the measurement of the loss tangent is not merely a direct measurement of acidity. It is quite probable that at least some of the oxidation products contributing to the dielectric losses have a polar structure without being acidic. This fact is borne out experimentally as shown by Figure 3.4. During the very early stages of oxidation, tan δ increases rapidly compared with acidity, indicating that the initial oxidation products are polar but not acidic. However,

except for this initial period, the quantity of acidic oxidation products formed in a particular oil increases more or less in step with the quantity of polarizable products giving rise to the dielectric losses.

It will be recalled that the aged samples of Oil 2 were more highly sludged than those of Oil 1 and hence, one might be led to believe that the higher values of tan δ for Oil 2 were caused by the extra sludge. This conclusion would not be correct. The loss tangent measurements made on the oils from which the sludge had been removed by filtration, showed no decrease in tan δ. In fact, a slight increase was noted in some cases but this was undoubtedly due to inadvertently contaminating the samples with water, or some other polar impurity, during the filtration process. It must therefore be concluded that the sludge particles themselves do not make a significant contribution to the value of loss tangent measured with the technique employed.

The foregoing analysis does not necessarily imply that the sludge content of an oil and the measured loss tangent are not related. It is quite possible that these two quantities may be related indirectly. For instance, an oil showing a tendency towards sludge formation might also tend to form other oxidation products (not necessarily acids) having high polarization losses. In this way, a high loss tangent might be indirectly indicative of a high sludge content even though the sludge itself is not responsible for the dielectric losses. The experimental evidence suggests this proposal as a possibility but it has not been adequately demonstrated.

A possible reason for the negligible contribution of the sludge to the polarization losses is that the insoluble particles settle out rapidly to the bottom of the cavity where the E-field is weak. Thus, even if the structure of the particles happens to be polar, the dielectric losses associated with them will be small. If the particles could be placed in a region of high E-field, possibly by a different mode choice, the losses measured would probably be larger. However, it is felt that the losses caused directly by the presence of the sludges would still be a small percentage of the total. This observation is based partially on the relatively small effect which sludge removal had on the acidity of the samples.

Because the inhibitors added to transformer oils are often polar compounds, the initial loss tangent measured for new oils may vary over a considerable range. This aspect was not investigated in detail but a few measurements on new oils were made. An uninhibited oil had a loss tangent of 11.3×10^{-4} while a heavily inhibited oil, known to be of high quality, had a tan δ value of 14.1×10^{-4}. As a result, it is clear that a measurement of loss tangent, when applied to new oils, cannot be used as a criterion of quality.

At a frequency of 8.5 Gc/s, the loss tangent and dielectric constant of water are approximately 0.5 and 65 respectively. Test III was able to show that the presence of water did produce a measureable increase in tan δ but the magnitude of the increase was small. This is explained by noting that the solubility of water in a new oil is low, being of the order of 75 parts per million (ppm). For a used oil containing

moisture-absorbing material such as cellulose fibres or hydrophilic oxidation products, a somewhat higher moisture content is possible but the increase in tan δ caused by the water would still not be large. It may therefore be concluded that the increase in tan δ in aged or used oils is caused primarily by polarizable substances other than water.

The changes in the dielectric constant caused by the ageing or by the presence of water were of no significance for any of the oils tested. Even contamination with a material of high dielectric constant such as water, produced a change in ϵ_r which was small enough to be masked by the experimental error. This seems at first to be somewhat surprising but it is fully predictable if one considers a contaminated or oxidized oil to be the normal oil, loaded with small particles having a different dielectric constant. Lewin[26] gives an equation for calculating the effective bulk dielectric constant of a particle-loaded dielectric:

$$\epsilon_r = \epsilon_{ro} \left\{ 1 + \frac{3\left(\frac{v}{V}\right)}{\frac{\epsilon_p + 2\epsilon_{ro}}{\epsilon_p - \epsilon_{ro}} - \left(\frac{v}{V}\right)} \right\} \qquad \ldots 3.3$$

where

ϵ_r = effective bulk dielectric constant of the particle-loaded material,

ϵ_{ro} = dielectric constant of the main material,

ϵ_p = dielectric constant of the particles,

$\left(\frac{v}{V}\right)$ = ratio of total particle volume to total volume.

Equation 3.3 may be used when the radius of the particles

is very much smaller than the wavelength in the dielectric. Applying the equation to a transformer oil containing water particles, it is seen that a concentration of approximately 800 ppm would be required to produce a change in the dielectric constant of 0.25%. It follows that the much smaller concentrations of water found in practice do not produce a measureable change in ϵ_r.

Since the oxidation of an oil affects only a small percentage of the hydrocarbon molecules, leaving the others unchanged, the same argument may be used to show that the bulk dielectric constant should be affected only slightly by the ageing process. This was borne out experimentally by the measurements made on the artificially aged oils. The service-aged oils examined in Test IV showed a considerable variation in ϵ_r with the most severely deteriorated oil having the highest dielectric constant. It is felt that this is coincidental. The values of ϵ_r that were measured are probably determined by the original dielectric constant of each oil rather than by the degree of deterioration.

The technique employed for measuring the dielectric losses at X-band produced very good results. The most serious experimental difficulty encountered when first trying out the method consisted of ghost-mode interference in the partly filled cavity. This problem could be reduced by using a cavity with a smaller diameter, say for instance, 2.1 inches. The guide wavelength corresponding to a frequency of 8.5 Gc/s would then be 2.35 inches and only 6 modes could be propagated in the air-filled cavity. When partially filled with a material whose

dielectric constant is 2.15, an additional 5 ghost modes could exist. The dielectric depths corresponding to the excitation of these ghost modes could be avoided much more easily in this cavity than in the larger diameter cavity.

Because of the longer guide wavelength of 2.35 inches, the cavity barrel should be made longer and a micrometer whose travel is not less than 4 inches is recommended. The detailed design should be worked out so that with the desired depth of dielectric in the cavity, the tuning plunger is capable of being adjusted to yield any of the resonances, TE_{012} to TE_{014} inclusive. The theoretical unloaded Q of these resonances would be between 18,000 and 22,000 in a brass cavity at 8.5 Gc/s. This cavity design would permit the same type of measurements to be made with a considerable reduction in the mode-interference problem.

4. CONCLUSIONS

The significance of the microwave-frequency dielectric-loss measurement when applied to the evaluation of aged transformer oils has been investigated.

The technique of using a TE_{01}-mode cylindrical cavity, containing a depth of oil corresponding to one-half wavelength, proved to be a very satisfactory method of measuring the dielectric losses at X-band. The Q-measurement technique employed was sufficiently sophisticated to reduce the random error in the measured loss tangent values to less than 1.5%. The absolute error in the loss tangent values is less than 6%.

It has been established experimentally that the loss tangent of transformer oils, measured at X-band, increases as the oil deteriorates through oxidation. The increase in loss tangent closely parallels the increase in acidity but also depends on other factors such as the nature of the oil and the conditions under which the oxidation takes place.

Sludge particles, when present in an aged transformer oil, do not in themselves cause a significant increase in the dielectric losses. The possibility of an indirect relationship between the loss tangent and the sludge content of an oil is indicated but has not been established.

The change in the dielectric constant of an oil, caused by the presence of dissolved water, or by the artificial ageing process, is too small to be measured by the method used. A small but measureable increase in the loss tangent is produced by the presence of water in concentrations of approximately 75 parts per million.

APPENDIX

Evaluation of the Stored Energies

From Equation 2.23, the expression for the dielectric-stored energy U_d is given by

$$U_d = \frac{1}{2}\,\epsilon_d \int_{\text{Dielectric Volume}} |E|^2\, dv \qquad \ldots \text{A.1}$$

Substituting the value for the electric field given by Equation 2.13b into Equation A.1 and referring to Figure 2.6, the foregoing equation becomes

$$U_d = \frac{1}{2}\,\epsilon_d \int_{z=0}^{\ell_d} \int_{r=0}^{a} C_d^{\,2}\left(\frac{\omega\mu}{k}\right)^2 J_1^{\,2}(kr)\, \sin^2 \beta_d z_1\, 2\pi r\, dr\, dz_1 \qquad \ldots \text{A.2}$$

The depth of the dielectric is chosen so that $\ell_d = n_1\left(\frac{\lambda_d}{2}\right)$ and $\ell_t = n_2\left(\frac{\lambda_t}{2}\right)$ where n_1 and n_2 are integers.

Noting that $J_1(ka) = 0$ for the TE_{01} mode, Equation A.2 integrates[27] to yield

$$U_d = \pi\epsilon_d\, C_d^{\,2}\left(\frac{\omega\mu}{k}\right)^2 \frac{a^2}{2}\, J_o^{\,2}(ka)\, n_1\left(\frac{\lambda_d}{4}\right) \qquad \ldots \text{A.3}$$

A similar integration for the air-stored energy gives the following result:

$$U_t = \pi\epsilon_o\, C_t^{\,2}\left(\frac{\omega\mu}{k}\right)^2 \frac{a^2}{2}\, J_o^{\,2}(ka)\, n_2\left(\frac{\lambda_t}{4}\right) \qquad \ldots \text{A.4}$$

For the dielectric depth chosen, an inspection of Equation 2.15 shows that

$$\frac{C_t^{\,2}}{C_d^{\,2}} = \frac{\lambda_t^{\,2}}{\lambda_d^{\,2}} \qquad \ldots \text{A.5}$$

and hence

$$\frac{U_t}{U_d} = \frac{n_2}{n_1 \epsilon_r} \frac{\lambda_t^3}{\lambda_d^3} \qquad \text{... A.6}$$

where ϵ_r is the dielectric constant ϵ_d/ϵ_o.

Evaluation of the Wall Losses

The wall losses are calculated from Equation 2.24:

$$P_w = \frac{1}{2 \Delta_e \sigma_e} \int_{\text{Wall Area}} |H_T|^2 \, ds$$

On the side wall in the dielectric, $H_T = H_z = C_d J_o(ka) \sin \beta_d z_1$. Therefore, the side-wall loss in the dielectric is given by

$$\frac{1}{2 \Delta_e \sigma_e} \int_{z=0}^{\ell_d} C_d^2 \, J_o^2(ka) \sin^2 \beta_d z_1 \, 2\pi a \, dz_1$$

Integrating, the side-wall loss in the dielectric is equal to

$$\frac{C_d^2 \, J_o^2(ka) \, \pi a \, n_1 \lambda_d}{4 \Delta_e \sigma_e} \qquad \text{... A.7}$$

On the end wall in the dielectric, $H_T = H_r = -C_d(\frac{\beta_d}{k}) J_1(kr)$. Therefore, the end-wall loss in the dielectric is given by

$$\frac{1}{2 \Delta_e \sigma_e} \int_{r=0}^{a} C_d^2 (\frac{\beta_d}{k})^2 \, J_1^2(kr) \, 2\pi r \, dr$$

Integrating, the end-wall loss in the dielectric is equal to

$$\frac{\pi a^2}{2 \Delta_e \sigma_e} (\frac{\beta_d}{k})^2 \, C_d^2 \, J_o^2(ka) \qquad \text{... A.8}$$

In the air-filled section of the cavity, the wall losses are calculated in a similar manner by starting with Equation 2.24 and using the expressions for H_T which apply in the air-filled portion. The results are as follows:

The side-wall loss in the air-filled portion is equal to

$$\frac{C_t^2 J_o^2(ka)\pi a\, n_2 \lambda_t}{4 \Delta_e \sigma_e} \qquad \ldots \text{ A.9}$$

The end-wall loss in the air-filled portion is equal to

$$\frac{\pi a^2}{2 \Delta_e \sigma_e} \left(\frac{\beta_t}{k}\right)^2 C_t^2 J_o^2(ka) \qquad \ldots \text{ A.10}$$

The total wall loss in the cavity is obtained by summing the quantities A.7 to A.10. Using the relation $\frac{1}{k} = \frac{\lambda_c}{2\pi}$ to simplify the resultant expression, the total wall loss is given by

$$P_w = \frac{\pi a \lambda_d C_d^2 J_o^2(ka)}{4 \Delta_e \sigma_e} \left[n_1 + n_2 \frac{\lambda_t^3}{\lambda_d^3} + 4a \frac{\lambda_c^2}{\lambda_d^3} \right] \ldots \text{ A.11}$$

The quantity $\frac{1}{\Delta_e \sigma_e}$ is determined from a measurement of the unloaded Q of the cavity. For the empty cavity of length ℓ_o such that $\ell_o = \nu \left(\frac{\lambda_t}{2}\right)$ where ν is an integer, the stored energy is obtained from Equation A.4 and is equal to

$$\pi \epsilon_o C_o^2 \left(\frac{\omega\mu}{k}\right)^2 \frac{a^2}{2} J_o^2(ka)\, \nu \left(\frac{\lambda_t}{4}\right) .$$

The wall loss in the empty cavity may be obtained from the quantities A.9 and A.10 and is equal to

$$\frac{C_o^2 J_o^2(ka)\pi a \nu \lambda_t}{4 \Delta_e \sigma_e} \left[1 + \frac{4a \lambda_c^2}{\nu \lambda_t^3} \right].$$

Since $Q_o = \omega \frac{\text{Stored Energy}}{\text{Wall Losses}}$, it follows that

$$Q_o = \omega \epsilon_o \left(\frac{\omega\mu}{k}\right)^2 \frac{a}{2} \Delta_e \sigma_e \left\{ \frac{1}{1 + \frac{4a \lambda_c^2}{\nu \lambda_t^3}} \right\} \qquad \ldots \text{ A.12}$$

Equation A.12 is used to eliminate the quantity $\frac{1}{\Delta_e \sigma_e}$ from

Equation A.11, with the result:

$$P_w = \frac{1}{Q_o}\,\omega\varepsilon_o\left(\frac{\omega\mu}{k}\right)^2 \frac{a^2}{2}\,\frac{\lambda_d}{4}\,\pi C_d^{\,2}\,J_o^{\,2}(ka)\left\{\frac{n_1 + n_2\,\dfrac{\lambda_t^{\,3}}{\lambda_d^{\,3}} + 4a\,\dfrac{\lambda_c^{\,2}}{\lambda_d^{\,3}}}{1 + \dfrac{4a\,\lambda_c^{\,2}}{\nu\,\lambda_t^{\,3}}}\right\} \qquad \ldots \text{ A.13}$$

The quantities P_w, U_d and U_t/U_d are now available for substitution into Equation 2.21.

REFERENCES

1. Rogers, A. G., "Insulating Oils from Petroleum", Unpublished Report, Imperial Oil Limited, Toronto, 1963.

2. Morton, F. and Bell, R.T.T., "The Low Temperature Liquid Phase Oxidation of Hydrocarbons: A Literature Survey", J. Inst. Petrol., Vol. 44, 1958, p.260.

3. Thompson, C. N., "Mechanism of Copper Catalysis in Insulating Oil Oxidation", J. Inst. Petrol., Vol. 44, 1958, p.295.

4. Wood-Mallock, J. C., Steiner, H. and Wood, L. G., "The Effect of Metals on Transformer Oils and Some Methods of Protection Against Adverse Effect", J. Inst. Petrol., Vol. 44, 1958, p. 320.

5. McConnell, T. A., "Evaluation of Laboratory Tests as Indicators of the Service Life of Uninhibited Electrical Insulating Oils", Symposium on Insulating Oils, ASTM Special Technical Publication No. 218, 1957, p.3.

6. Gossling, P.W.L., In General Discussion, Symposium on Insulating Oils, ASTM Special Tech. Pub. No. 218, 1957, p.34.

7. Oliver, F. S., ibid., p.36.

8. Stark, K. H., "Dielectric Loss of Insulating Oil", Proc.I.E.E., Vol. 100 IIA, 1953, p.89.

9. Martin, R. G. and Patterson, E. A., "The Measurement of the Power Factors of Insulating Liquids at 50 c/s", Proc.I.E.E., Vol. 100 IIA, 1953, p.68.

10. Bennett, G. E., "Electrical Measuring Techniques and their Application to Insulating Oils", J. Inst. Petrol., Vol. 44, 1958, p.361.

11. Childs, D. G. and Stannett, A. W., "Some Aspects of the Deterioration of Insulating Fluids", Proc. I.E.E., Vol. 100 IIA, 1953, p.61.

12. Salomon, T., "Correlation Between Dielectric Loss and Chemical Stability of Mineral Oils", Paper presented at the Symposium on Liquid Dielectrics, Electrochemical Society, Philadelphia, May 1959.

13. Debye, P., Polar Molecules, Chemical Catalogue Company, New York, 1929.

14. Smith F. E., "Dissipation Factor Measurements of Transformer Oil", M.A.Sc. Thesis, Department of Electrical Engineering, The University of British Columbia, 1951.

15. Dekker, A. J., Solid State Physics, Prentice-Hall, Inc., 1957, p.151.

16. Walker, G. B. and Luthra, S. P., "Limitations of Methods for Determining Dielectric Properties by the use of a Standing-Wave Indicator", Proc. I.E.E., Vol. 109 B, Supp. No. 23, 1962, p.651.

17. Free, J. M. and Walker, G. B., "Determination of the Dielectric Properties of Low-Loss Ceramics at Q-Band Frequencies", Proc.I.E.E., Vol. 107 B, 1960, p.354.

18. Bleaney, B. and Loubser, B., "Cavity Resonators for Measurements with Centimeter Electromagnetic Waves", Proc. Phys. Soc. London, Vol. 59, 1947, p.185.

19. Ginzton, E. L., Microwave Measurements, McGraw-Hill Book Company, Inc., 1957, p.394.

20. Ginzton, E. L., ibid., p.406.

21. Lamont, H.R.L., Waveguides, Methuen's Monograms, John Wiley and Sons, Inc., 1951.

22. Slater, J. C., Microwave Electronics, D. van Nostrand Company, Inc., 1950, p.48.

23. Penrose, R. P., "Some Measurements of the Permittivity and Power Factor of Low-Loss Solids at 25,000 mc/sec Frequency", Trans. Far. Soc., Vol. 42A, 1946, p.108.

24. Luthra, S. P., "Investigation into the Properties of Dielectrics for Microwave Tube Applications", Ph.D. Thesis, University of London, 1962.

25. ASTM Standards on Petroleum Products, American Society for Testing Materials, 1959, p.450.

26. Lewin, L., Advanced Theory of Waveguides, Iliffe and Sons, Limited, London, 1951, p.156.

27. Ramo, S. and Whinnery, J. R., Fields and Waves in Modern Radio, John Wiley and Sons, Inc., 1953, p.167.